THE ELECTROMAGNETIC VELOCITY GAGE AND APPLICATIONS TO THE MEASUREMENT OF PARTICLE VELOCITY IN PLASMA

By
David J. Edwards
John O. Erkman
Edmund J. Jacobs

20 JULY 1970

NAVAL ORDNANCE LABORATORY, WHITE OAK, SILVER SPRING, MARYLAND

THE ELECTROMAGNETIC VELOCITY GAGE AND APPLICATIONS TO THE MEASUREMENT OF PARTICLE VELOCITY IN PMMA

by:

David J. Edwards

John O. Erkman

Sigmund J Jacobs

ABSTRACT: The electromagnetic velocity (EMV) gage was used to investigate particle velocity vs. time and peak particle velocity vs. distance at several points in PMMA (polymethylmethacryiate) in the donor-gap arrangement of the NOL Large Scale Gap Test. The results obtained by the method agree favorably with previously measured peak particle velocities for gap distances from the HE-PMMA interface between 10 and 25 mm. At closer distances the particle velocity-time records are in good relative agreement with one dimensional hydrodynamic computations. The values of peak particle velocity found for distances less than 5 mm are not in agreement with the previous extrapolation to zero gap of the earlier data obtained for gaps $\geq$ 10 mm. Consequently, a new tentative calibration for the close-in distance is presented. The study encountered a number of recording problems; noise in the records and poor system response. Steps taken to eliminate the noise and to improve the recording response are outlined. Also discussed are the theoretical behavior of the gage, factors influencing system response, and comparison of real with predicted response. It was concluded that the EMV gage is a convenient and useful tool for measuring particle velocity vs. time in non-conducting or weakly conducting media.

PUBLISHED 20 JULY 1970

U.S. NAVAL ORDNANCE LABORATORY
White Oak, Silver Spring, Maryland

NOLTR 70-79 20 July 1970

THE ELECTROMAGNETIC VELOCITY GAGE AND APPLICATIONS TO THE MEASUREMENT OF PARTICLE VELOCITY IN PMMA

The work described in this report was carried out under Task IR-59, Transition from Deflagration to Detonation, of NOL's Independent Research Program. It is of importance to the effective use of explosives.

The work described is a study of an electromagnetic technique previously described in Russian reports for application to the measurement of particle velocity in detonating explosives and in shocks produced in non-conductors by explosives. Applications of this technique in this area of research has been largely overlooked in this country. Therefore, this study was undertaken at NOL to find out how precise and how useful the method might be. The results of this study confirm the Russian claims that the method is a valid approach to the study of shock waves and detonation waves. Reported are some results obtained with the Large Scale Gap Test used at NOL for the evaluation of the shock sensitivity of condensed explosives. It has been demonstrated that the calibration of the test must be revised for small gaps. The results of a previous calibration are, however, found to be satisfactory in the gap range usually encountered in sensitivity testing. An abbreviated version of this report was accepted for presentation at the 5th Symposium (International) on Detonation, Pasadena, California, 18-21 August 1970. The written version appears in the preprints of that symposium.

The identification of commercial materials implies no endorsement or criticism by the U. S. Naval Ordnance Laboratory.

GEORGE G. BALL
Captain, USN
Commander

J. E. ABLARD
By direction

CONTENTS

Contents (Continued)

TABLES

FIGURES

I. INTRODUCTION

A promising technique for the absolute measurement of particle velocity as a function of time in high amplitude shocks and detonations known as the electromagnetic method was introduced into the scientific literature by Zaitsev, Pokhil, and Shvedov[1] in 1960. In principle the method is a direct application of the Faraday law of electromagnetic induction. Simply stated, a measurement of particle velocity in a non-conducting, dense, fluid-like medium can be obtained from the emf developed across a thin metal foil or ribbon of known length moving with the fluid in a magnetic field of known strength oriented normal to the direction of the ribbon and the direction of the motion. When the foil length is ℓ cm, the field strength is H gauss, and the velocity of the ribbon is equal to the flow velocity u in mm/usec, the generated emf in volts is given by

$$V = 10^{-3} \cdot H \cdot \ell \cdot u \quad . \qquad (1)$$

Electromagnetic velocity (EMV) gages constructed on the above principle have, in recent years, been one of the basic instrumental techniques for a number of papers on shock wave and detonation wave flow and pressure determination[1-13]. Except for four papers the work is all of Russian origin, and most of these are by Dremin or his associates. The Russian applications of the method are of considerable importance to the study of explosives behavior. For example, the results reported on reaction zone length and detonation pressure raise the question of misinterpretation of free surface velocity measurements by American researchers. In particular Dremin, et al[10] have reported C-J pressures for Composition B which are about 10% lower than the findings of Duff[14] and of Deal[15]. Dremin has argued that these workers selected the incorrect point in the observed free surface velocity vs. distance curve as the value to be related to the C-J point. The work of Dremin strongly suggests, in agreement with Petrone's arguments[16], that Craig[17] may also have chosen a high value for the C-J pressure for TNT and nitromethane. The "failure" of the C-J theory suggested by Davis, et al[18] may, in fact, be an error of interpretation of observations on free surface velocities. Further study, with the magnetic method for support, may be able to clarify the point of disagreement.

There is enough evidence in the Russian work to make it clear that the EMV gage could be a powerful tool for the solution of many problems in explosives. The fact that it gives particle velocity directly as a function of time is sufficient reason for giving the method serious consideration. The free surface velocity methods, by contrast, measure distance and time. These x-t data yield only the initial value of particle velocity, not u(t). Another approximately direct method for determining shock wave particle velocity is the quartz gage. This method is not useful above 50 kb in quartz; moreover, it requires conversion of data through assumed impedance relationships. Other known gages used for shock pressure (and hence particle velocity) measurement are of the indirect type requiring pressure calibration with known experimental pressures. They are therefore less suitable for precise experimentation.

In 1966, after a brief paper study,[19] it was suggested that NOL undertake to check out the method with a system for which data were already available for comparison of results. The HE donor - PMMA gap material of the NOL Large Scale Gap Test (LSGT) provides such a system. Consisting of a tetryl donor charge of 5-cm diameter, 5-cm length, and a PMMA (Plexiglas) gap of variable length, this system has been calibrated by Price and Liddiard[20,21] to obtain peak pressure as a function of PMMA thickness. In the latter work, free surface velocity measurements were made with a smear and a framing camera. By use of the usually accepted approximation that particle velocity is half the free surface velocity, data are available on peak particle velocity over the range 0.10 to 1.42 mm/usec (PMMA gaps, defined by **X**, $\geq$10 mm). The system is small enough to employ the EMV gage method with a moderate size magnet having a pole face spacing of 8-10 cm. Since the EMV method permitted studies in PMMA to be made closer to the HE interface than reported in reference (21), measurements were made over the range **X** = 0.25 to 25 mm from the HE-PMMA interface.

It was decided, in advance, that an initial test should be made on an inert plastic rather than an explosive in order to avoid a possible error in the measurement which could arise from the conduction of the moving particles in a detonation. PMMA is inert in the sense that it does not become conducting under shock, but it happens to generate a piezoelectric (PE) signal under shock.[8,23,24] In practice the PE signal appears to cancel in the EMV gage arrangement and cause no trouble. Noise which was apparently due to the detonating explosive was observed on the records. We were able to minimize this signal by changes in the experimental set-up and by increasing the field from 400 gauss to about 1400 gauss. With these changes, agreement with the peak particle velocity results of Price and Liddiard was obtained to between 2 and 4%. At present we are not sure which experiment is the more accurate. In addition, the particle velocity as a function of time was obtained for all EMV shots.

In the Russian work cited, the rise-time for an experiment was quoted to be 60 to 100 nanoseconds with very little rounding off of the front of the recorded signal. (The term "rise time" appears to be a matter of translation from the Russian. The time referenced is probably time to maximum response.) Some of our earlier records, however, had much longer time to maximum (200-300 ns). Severe round-off of the signal affected our results at distances where the effects of the reaction zone and the steeply decaying Taylor wave of the explosive were still apparent in the PMMA ($x < 4$ mm). Our results at $x = 4$ mm and larger were not affected because the above interactions had vanished and the particle velocity vs. time fall-off was essentially linear. The rounding-off was found to be a result of circuitry. This problem has been corrected insofar as possible as will be discussed in Section V. The time to maximum for our best recording set-up is now as short as 20 to 40 ns.

This report discusses (a) the experimental donor-gap set-up; (b) the EMV gage method and how it is experimentally incorporated into the experiment; (c) recording problems; (d) the results of our measurements; and (e) comparisons with other related work.

II. THE EXPERIMENTAL SET-UP

A. Charge-PMMA Configuration

For all experiments the explosive charge and PMMA gap arrangement, Fig. 1, was that used by Liddiard and Price,[20,21] the arrangement of the NOL standard Large Scale Gap Test. The donor explosive was a cylinder of graphited tetryl, 5.08 cm diameter by 5.08 cm long. The explosive is a pressed charge at a density of 1.51 ± 0.01 gm/cc. Its measured detonation velocity is 7.2 mm/μsec. In this work the tetryl was point initiated by using a primacord lead (120 grain/foot, RDX) 30 cm long initiated by an SE-1 detonator. The detonator, which is of the high voltage PETN exploding bridge wire (EBW) type, was used for reasons of safety in the presence of the relatively high magnetic fields. The primacord lead is then used to isolate the charge and prevent possible stray pick-up in the EMV gage due to the electrical signal from the firing unit. All PMMA samples which determine the gap between the HE and the gage were machined from cast PMMA rods of 5.08 diameter and of length, X, from 0.25 to 25 mm. The density of the PMMA is 1.18 ± 0.01 gm/cc. The Hugoniot U-u for the PMMA at U > 0.5 mm/μsec taken from previous work[20] is

$$U = 2.56 + 1.61 \cdot u \qquad (2)$$

where U and u are respectively the shock and particle velocity in mm/usec. The Hugoniot pressure (in kilobars) can then be obtained from the momentum conservation relation

$$P = 10 \cdot U \cdot u \cdot \rho_0 \quad . \qquad (3)$$

The EMV gage consists of a rectangular loop of aluminum foil 0.013 mm (0.5 mils) thick and 2 mm wide. It is mounted in a PMMA back-up assembly whose thickness F is 12.7 mm, see Fig. 1. The voltage is generated when the base of the gage moves in a magnetic field. The length of the base, ℓ, is determined by the width (5 or 10 mm) of piece A in the experimental set-up shown in Fig. 1b. The assembly of the back-up is made by cementing two blocks B to the spacer block A by softening the PMMA surfaces with chloroform,

after which they are clamped together and similarly cemented to the gap section C and held until the bond hardens. Care is taken to eliminate air bubbles, especially in the vicinity of the pick-up. The gage circuit is completed by connecting the foil leads (32-34 mm length) to a coaxial line (RG58C/U, nominal impedance of 50 ohms). Some of the shots had a 50 ohm resistor in series with the foil; this will be discussed fully in Section IV. The ionization switch to trigger the scope, shown in Fig. 1, consisted of two strips of aluminum foil placed about 3 mm apart on the explosive charge about 25 mm below the PMMA interface. The trigger signal is fed to the oscilloscope on a coaxial line.

A baffle, shown in Fig. 1, was located in the plane of the HE-PMMA interface. It consisted of a 7.5 cm square piece of aluminum, 0.64 mm thick, with a 5.08 cm circular cut-out. The significance of this baffle will be discussed in Section IV-C.

B. Magnets

Two magnet arrangements were used in the experiments. Initially Helmholtz coils of nominal diameter 24 cm spaced 12 cm apart and having 400 turns of No. 16 wire were used. These with the available power supplies (12 amps in each coil) give a uniform field of about 300 gauss at the center of symmetry. An iron core magnet was later used to obtain a larger field (approximately 1400 gauss, maximum), see Fig. 2. This magnet has circular pole faces of 10.2 cm diameter spaced 8-10 cm apart. The field uniformity in the vicinity of the mid-plane as measured at a lower field strength is ±0.6%. The magnet was not severely damaged in the experiments and could be used repeatedly. A field calibration was made before each experiment. The pole faces were protected by 1/4 inch wood baffles. These baffles not only protected the pole faces from damage from the blast but also prevented undesirable stray fields which are otherwise generated when the conducting air shock moving in the magnetic field strikes the conducting pole faces.

III. THE ELECTROMAGNETIC VELOCITY GAGE METHOD

A. Theory

A general description of the EMV gage method and its instrumentation requirements has been described in cited reports. Reference 19 summarized this information. We will discuss here the background information which is needed for the description of the present experiments. First, we note that the gage circuit is a single turn rectangular loop of conducting foil closed by a resistance R (Fig. 3). R may be the characteristic impedance of a coaxial line which connects the loop to an oscilloscope. (The line is terminated at the far end by an equal resistance.) When a series resistor is employed, R is the sum of its resistance, the characteristic resistance of the terminated line, and the resistance of the terminator. By Faraday's law of induction, there will be an emf generated across R whenever the magnetic flux within the loop is changed, that is

$$V = -d\Phi/dt \tag{4}$$

where Φ is given by the scalar product

$$\Phi = \vec{H} \cdot \vec{A} \tag{5}$$

H being the magnetic field strength and A the cross sectional area enclosed by the loop. When H is constant and normal to the plane of the loop, changes in Φ arise only from changes in A. If one side (the base) of the loop is moved normal to itself thus reducing A, Eq. (4) reduces to Eq. (1) (see also Fig. 3b). Precisely speaking, then, the method applied to shock particle velocity measurement requires the following conditions to be satisfied:

(a) the gage base of length ℓ must move with the (parallel) flow in the system in a direction normal to the field and

(b) to prevent additional voltages from being generated all other parts of the loop must either remain stationary or move in such a way that they do not cut the field. That is, the two arms connecting to the base can move in the direction of the flow, i.e., contract, without modifying the voltage (Fig. 3a).

These conditions underlie the statement that the shock wave should be plane and move normal to the field; the EMV gage base should be parallel to the shock front and normal to the field; and the connecting leads should be normal to the shock front. We should point out here that the discussion of the gage in terms of a loop helps in the consideration of background noise. If, for example, the explosion causes any asymmetric flow of electrons or ions, the flow could generate magnetic fields which alter ϕ. This would be picked up by the loop. Signals of this type could be minimized by making the loop as small as possible.

An idea of what happens when the end of a loop is intercepted by a divergent shock is shown in Fig. 3c. First the curved shock intercepts the midpoint of the gage base setting it into motion; after a time given approximately by

$$\tau_c = \ell^2/(8 \cdot r_o \cdot U) \qquad (6)$$

where U is the shock velocity and r_o is the radius of curvature of the shock front, the ends of the gage begin to move. When the shock has passed to $r > r_o$, we can assume the gage ends to have moved on radial lines from b to b' and from c to c'. The leads, though perhaps not displaced exactly as shown, will nevertheless be displaced approximately to ab' and dc'. Thus, the reduction in area of the loop will be slightly less than that which would have occurred in a plane flow; an underestimation of the velocity results. If r_o is large, however, compared to ℓ and all measurements are made while $r - r_o$ is small compared to ℓ the error in assuming $dA/dt = u\ell$ will be small. The error in dA can be estimated and a correction made if desired. We have neglected the correction in this report.

B. Factors Influencing Oscilloscope Measurements

Given an ideal situation where the medium is non-conducting and not generating spurious signals as a result of shock polarization or other causes there still remain at least 5 specific factors which can lead to records which do not faithfully reproduce the flow in the medium. These are:

(a) Wave front curvature as just discussed,
(b) Shock impedance mismatch between the sensing foil and the medium,
(c) Inherent response or rise-time from the oscilloscope,
(d) Wave front tilt, and
(e) Electrical impedance mismatch between the coaxial line and the oscilloscope or the magnetic loop.

These factors pertain chiefly to the response of the system in the time period shortly after shock arrival at the base of the gage.

In principle the coaxial line presents a resistive load R_c to the magnetic loop. If the line is then properly terminated at the scope (with a resistance equal to R_c) no response error should be introduced by the line. The line would merely delay the recording signal. In practice it was found on a high frequency response oscilloscope that simple termination at the oscilloscope cannot be realized. The internal characteristics of the oscilloscope led to a reflection of part of the initial signal which showed up as a "ringing" on the oscilloscope trace. As a consequence the resistance R_1 of Fig. 3a was added to reduce the ringing when this oscilloscope was used. No ringing was seen when the lower frequency response oscilloscopes were used. Details concerning the method of selecting R_1 are discussed in Section IV.

In the consideration of the effect of electronic circuit elements on the response signal recorded on an oscillograph it is customary to assign a rise-time to each circuit element (including the oscilloscope). An accepted definition of rise-time T is the time for the response from a square-step input to rise from 10% to 90% of maximum response amplitude. For a simple RC circuit (shunt capacitance) the rise time so defined is 2.20 times the circuit time constant, $\tau = R \cdot C$. When several circuits are used there is a convenient approximation for the overall rise time, T_o, in terms of the rise times of individual elements, T_i, which is

$$T_o = (\Sigma T_i^{\,2})^{1/2} \quad . \tag{7}$$

In many shock measuring problems the expected wave-form is far from a square step. The particle velocity is like a step jump followed by a linear or exponential decay. The response to such a wave-form will be a record with rounding at the top of the trace having a time to maximum which will depend on the effective τ or T_o of the measuring system and on the rate of decay of the flow in the medium being studied.

An example of the response of an oscillograph to an exponentially decaying input function has been given by Cole[25] in connection with the problem of measuring underwater shocks with a piezoelectric gage. The response to a triangular input when a simple RC circuit is used to simulate the recording elements has been worked out in Appendix A for several decay rates. Times to maximum T_{max} range from 2.5 τ to about 5 τ (1 - 2 T_o) and times to approximately linear response T_{lin} run about 4.5 τ (2 T_o).

To check on Eq. (7) the problem of square-wave response with 2 time constants has been solved for several cases (time constants in the ratio 0.1 to 2). The result agrees only qualitatively with Eq. (7), but indicate that Eq. (7) is sufficiently good for purposes of estimating. The solution is given in Appendix B.

In the present work three of the sources of response error are non-electrical elements. For each of these we must estimate a time T_i from 10% to 90% of maximum response to be used in Eq. (7) for an overall response estimate. The time at which 90% of the gage would be set into motion, in the absence of inertial effects is seen from Eq. (6) to be 0.81 τ_c. We therefore define T_1 as 0.8 τ_c as sufficiently close for the wavefront curvature rise time. The effect of wave front tilt would be treated in a similar manner if we had some basis for determining the tilt. In our work, this information is lacking and no a priori tilt effect on rise is possible. The effect of shock impedance mismatch between the medium and the foil can be given a rise-time value T_2 by considering the motion of a foil subjected to a square-step shock in the medium. It should be sufficiently accurate for this purpose to use a linear approximation to establish the time it takes to get the foil up to 90% of the velocity of the medium. Figure 4 shows the p-u states which will be obtained for PMMA and aluminum (assumed impedances 5 and 16 mm-g/cm^3-μsec). The result gives an estimate of 2 double transit times in the aluminum (at about 6 mm/μsec) to reach (in fact, to exceed) 90% of the velocity of the medium. Two double transits are therefore used as the effective acceleration rise-time T_2. Estimates of overall rise-time for our experimental set-ups are given in Section IV-D.

IV. RECORDING INSTRUMENTATION, NOISE, RESPONSE, AND REPRODUCIBILITY OF RECORDS

Notwithstanding the fact that Russian workers have written numerous reports on the EMV gage method, they have given very little information about details of the instrumentatior which they used. We have found but one statement to the effect that the rise-time was about 100 ns. At first sight the recording problem appeared to be straightforward and simple. When we started to make measurements, however, we found ourselves confronted with a number of problems which had to be solved before good records could be obtained. In this section the recording problems are discussed. The instrumentation and oscilloscope arrangements are first outlined to clarify the discussion.

A. Oscilloscope Arrangements

In the course of the work it was found necessary to make changes in the oscilloscope set-up to improve on the records. We started the study with two Hewlett-Packard Model 160 oscilloscopes having frequency response of 14 MHz (rise-time = 25 ns). These were connected in parallel with 2 feet of coaxial cable between the oscilloscopes. A Tektronix Model 011-49 50 ohm terminator was then connected to the last oscilloscope. We will refer to this set-up as Arrangement A. Because of the inability to obtain the expected response after many trials with this set-up one of the oscilloscopes was removed for a few experiments. The remaining oscilloscope was terminated as before. This is referred to as Arrangement B. To further improve on the response of the system a faster oscilloscope, a Tektronix Model 454, having a frequency response of 150 MHz (rise-time - 2.4 ns) was acquired. Used with the terminator of Arrangement B, this is called Arrangement C. In both Arrangements A and B the trigger signal for the oscilloscopes was obtained from the shorting of the ionization switch located on the tetryl charge, Fig. 1, connected by a coaxial line to the trigger pulser and the oscilloscopes. The trigger signal to the oscilloscopes was 30 volts obtained by a capacitor discharge in the pulser. The pulser was unnecessary for Arrangement C because the Tektronix oscilloscope contains an internal trigger with sufficient built in delay for the gage signal to be recorded.

In the case of Arrangements A and B the gage was connected directly to the 15 foot coaxial line to the oscilloscopes. When Arrangement C was first used it was found that a high frequency ringing appeared in the oscilloscope trace. This was traced to a small internal mismatch of impedance between the gage and the terminated line. This mismatch may have been present in the H-P oscilloscopes yet remain undetected because of the poorer response in those oscilloscopes. The ringing in the Tektronix application lasted about 80 ns (about 3 double transit times of the coaxial line). It was reduced to an acceptably low level by inserting a resistor R_1 in series with the gage at the gage end of the line, see Fig. 3a. The best value for R_1 was very close to the characteristic impedance of the cable, 50 ohms. It was checked by use at a H-P Model 1415A Time Domain Reflectometer with the gage in the circuit. With R_1 in the circuit, the gage output is reduced at the scope in the ratio $R/(R + R_1)$, R being the value of the terminating resistance at the oscilloscope.

B. Calibration Procedure

Voltage and time calibration marks were placed on all oscilloscope records. Voltage calibration was obtained by using a constant voltage generator, the output of which was measured with a Fairchild Model 7050 Digital Multimeter which has an accuracy of ±0.1%. Because of the high impedance of the generator (about 1 kohm/volt) the low impedance coaxial line and termination was removed during oscilloscope calibration. Time calibration was obtained from a crystal controlled time mark generator (Tektronix Model 180A). The magnetic field was measured with a Rawson-Lush type 824 rotating coil gaussmeter which has a calibration accuracy of ±1%. The magnets were energized by either a Perkins Model TV R 040-15 power supply with a maximum output of 45 volts and 16 amps, or by an ERA Magnitran, Model TR 36-8NL supply rated at 36 volts, 8 amps. Both these supplies were of the constant voltage type so there was no compensation for change of resistance and current as the coils became heated when energized. Error was minimized by taking flux reading in as short a time as possible and then shutting off the power. For the same reason, the power was again turned on only a few seconds prior to the shot. The constant voltage supply is not desirable and a constant current supply has been obtained so that the field can be controlled and measured more accurately.

The first step in preparing an experiment was to measure the magnetic field at the central point of the magnet where the EMV gage would be located. With the power to the magnet turned off the explosive charge was then placed in position and the detonator was connected. Current to the magnet was then restored to the original value and the standard firing procedure for firing explosive charges was followed.

C. Noise Elimination

The first source of noise anticipated in the records was electrical pick-up from the detonator firing circuit. The EBW detonator requires a large firing power supply; 6 microfarads charged to 2,500 volts. To eliminate the possibility of picking up noise from this large energy source the detonator was decoupled from the main charge by a primacord lead of sufficient length, 30 cm, to permit the electric field to dissipate before the event to be recorded took place.

Unanticipated noise in preliminary trials with Arrangement A was thought to be due to a magnetic signal generated by the air shock and explosive product gases from the tetryl booster moving outward and along the PMMA surface. To track down the source of this spurious signal, shots were fired with the same set-up as for velocity measurement but without energizing the magnet. The result was a 40 mv signal when the sensing base of the gage was at 19 mm from the HE-PMMA interface (see arrow on Fig. 5a). A baffle as shown in Fig. 1 was then tried. The resulting signal was still too large though somewhat reduced. Grounding the baffle to the trigger line shield reduced the noise to 2 mv (see arrow in Fig. 5b). Although the exact reason for the spurious signal is not clearly known, the signal was reduced to an acceptable level. Use of the grounded baffle became standard procedure, and the spurious signal has thereby appeared to be under control in all the work on PMMA which followed.

D. Measuring System Response

Section III-B outlined a procedure for estimating the overall rise time of the system consisting of the gage and the scope. Estimated numbers for the components in our experiments have been used to obtain predictions of response times. These are listed in Table I together with the input values used for the calculations based on Eq. (7). The effect of tilt of the shock wave relative to the base of the gage has not been determined yet and therefore is omitted. The results indicate that the time to maximum in the records for Arrangements A and B with a gage base length of 10 mm should be about 63 ns. With a fast oscilloscope, Arrangement C, and a 5 mm base length the predicted time to maximum is of the order of 17 ns. Comparisons with actual experimental values are discussed below.

Arrangement A - The original oscilloscope set-up produced records which showed severe round-off in the region of maximum response. The time, T_{max}, was typically about 140 ns for a gage base length of 5 mm. This is about three times as great as the estimate of about 50 ns. It was guessed that the trouble could have arisen from improper impedance matching of the scopes to the line. (In principle, the mode of connection appeared correct.) The apparent u-t curves obtained by converting the voltages to velocity are plotted in Fig. 6.

Arrangement B - This was used for the purpose of checking on the two-oscilloscope set-up above. This arrangement produced traces with T_{max} much closer to predicted values: 50 to 64 ns for the 5 mm base length. This agreement with the prediction is better than expected in view of possible errors in the rise time estimates. The improvement over Arrangement A suggests that the trouble with the original system was mismatch of the oscilloscopes to the coaxial line. The u-t curves for the Arrangement B set-up are plotted in Fig. 7.

Arrangement C - This is the most desirable oscilloscope set-up. It was not available when the experiments were started. The entries in Table 1 for this oscilloscope set-up show that the oscilloscope is no longer the critical factor for determining the rise time. In these experiments it is either wave front curvature or transit time for accelerating the foil. For a plane wave boostered experiment, it would be the foil acceleration time. The values found for T_{max} for a 5 mm base length are 20-31 ns. These numbers are not in good agreement with the calculated value, 17 ns. Wave tilt, if present, could probably account for the discrepancy. Tilt effect, however, should not be present on all records. Typical reduced records of u vs t are plotted in Fig. 7.

Examples of the oscillograms obtained with the three arrangements are shown in Fig. 8. The curves of Figs. 6 and 7 are discussed more fully in the following section.

The results of the response checks on the oscilloscope systems indicate that our best set-up, Arrangement C, is incapable of resolving data on particle velocity for times $\leq$30 ns. If the velocity is close to linear in the time for about 100 to 200 ns thereafter, then it is possible to extrapolate back to zero time to obtain a pretty good value for the initial particle velocity. If foils of thickness much greater than 13 microns are required, the resolution will suffer even if the shock wave is plane. In these experiments the particle velocity vs time is fairly linear when the thickness of PMMA exceeds 5 mm. Thus, for $X > 5$ mm the results on initial particle velocity obtained even with the poorer oscilloscopes are still expected to be quite precise.

E. Reproducibility of Records

Of a total of 44 experiments to measure particle velocity by the EMV gage, about 30 resulted in usable records which have been analyzed to obtain initial particle velocity. Records from some experiments were not usable for the following reasons:

Loss of voltage calibration	1 record
Loss of record	4 records
Excessive ringing in record	9 records

It is of some interest that no records were lost because of breakage of the foil in the gage itself. (We may have had cases of loss of response due to foil breaks at times greater than 1usec.) Most of the records lost due to ringing were on preliminary tests with the Tektronix oscilloscope made before the impedance mismatch at the oscilloscope was understood and a cure found for it. The above box score can be taken as an indication that, with experience, one should be able to attain a high percentage of successful experiments. In the recording of particle velocity within a PMMA sample with time base exceeding the time for the shock to reach the free surface, it was invariably found that the record went astray at the time the shock reached the surface. This is illustrated in Fig. 8a and a record is to be discussed later.

In Fig. 9 some of the u-t traces from Figs. 5 and 7 have been combined to illustrate the kind of reproducibility obtained in duplication of records at several given distances, X, from the HE interface. Unfortunately most of these duplications were obtained with the inferior oscilloscope arrangement. At X = 20 mm there is one good check between two records, one with Arrangement A and one with Arrangement C. For the comparative records (Arrangement A) it can be said that agreement is good after 400 ns. There is a fairly large scatter in rise time between records; consequently, in these early times reproducibility is poor. Those records which exhibit faster rise are taken to be the most reliable. In the Arrangement A it is unlikely that the differences in rise time can be attributed to tilt of the shock wave relative to the base of the gage. It can be noted that in spite of the poor response the records extrapolated quite closely to the same initial value of u for a given value of X and that the slopes after 500 ns are reproduced quite satisfactorily.

The lack of reproducibility of structure in the records taken with Arrangement A prompted a careful examination of all records available from Arrangement C. We found that two records, rejected for analysis because of ringing, contained useful information on reproducibility of the shape of the recorded wave. These records, shots number 92 and 97, were taken at X = 0.86 mm with a base length of 5 mm. Recording time exceeded 2 usec on both records. The records are reproduced in Figs. 10a and 10b. (Shot 92 was fired using an oscilloscope which was being demonstrated to us. It had a stated rise time of 7 ns.) The ringing in these records is confined to the initial rise and to two or three limited periods later in the records. The times at which ringing appeared on both records were the same. It is fairly well known that ringing can be excited in an undamped circuit when the input signal breaks sharply from one slope to another. It appeared, therefore, that both records were exhibiting sharp change in slope at times of about 300, 600, and 1100 ns. To verify this conclusion another shot was fired with Arrangement C taking all possible precautions to obtain good termination of the coaxial line. This record,

number183, is reproduced in Fig. 10c. Note that Fig. 8c shows a record shot 108 made with a shorter time base under the same conditions. The four records taken with the fast oscilloscopes and one under similar conditions with the slow rise oscilloscope have been reduced to u-t plots which are shown in Fig. 11. The curves have been displaced relative to each other so that they can be more easily compared. We note that shots 97 and 92 agree in shape out to a time of 1.2 μsec though shot 97 is low by about 10%. The latest record, number 183, agrees in shape and amplitude with number 92 to 1.3 μsec insofar as the latter can be measured. The slopes of the traces beyond 1.2 μsec differ so that we are left in doubt as to which is the more correct. We are now of the opinion, in view of the agreement of trace shapes, that there was a calibration error in shot 97. Shot 183 can be interpreted as having breaks in the curve at times about 260, 660, and 1330 ns. These breaks are more or less confirmed by the other records; the last time is closer to 1100 or 1200 on the earlier records. In shot 108 we note that a ringing signal is evident, starting at about 260 ns. This can be interpreted as evidence of a break in slope. The time is that for the first break in shot 183. Although these are not perfect examples, we believe they demonstrate that it is possible to refine the EMV method to give us a useful tool for the measurement of particle velocity as a function of time in this non-conducting medium. The intermediate lower slope in the record at X = 0.86 mm between 660 and 1330 ns gives reason to believe that the observed concave downward shape of a few of the previous records is, indeed, real. The downward inflection of curve 3 in Fig. 6 appeared to be erroneous when it was first plotted. The normally accepted picture of the particle velocity-time curve in an explosive driven shock is that the u-t curve would be concave upward. When we note that the inflection at about 800 ns in Fig. 6c is at a particle velocity of about 1.4 mm/μsec, we see that the 800 ns inflection relates satisfactorily to the 1300 ns inflection for X = 0.86 mm. Admittedly, we cannot yet explain all that we observe in the records. The structure within the waves and how it may develop is a problem for future consideration. In the next section the results obtained for peak particle velocity are examined in the context of other work.

V. RESULTS OF MEASUREMENTS

A. Comparison with Free Surface Velocity Measurements, X ≥ 10 mm

The Donor-PMMA system used here was previously investigated by Liddiard and Price[21] for the purpose of calibrating the Large Scale Gap Test. Their measurements of free surface velocity extended over the range X = 10 to 150 mm. In that work the initial particle velocity of the shock in PMMA was taken to be half the initial free surface velocity measured at a given distance from the HE interface. Our measurements were made for X ≥ 0.25 mm and overlap the earlier work in the range 10 to 25 mm. Most of our data in the overlap range were obtained in the early part of our work. Although the system response at that time left much to be desired, the rate of decay of the particle velocity was sufficiently low and sufficiently linear that an accurate extrapolation of each record back to the time of arrival of the shock was possible. The extrapolation was accomplished by a straight line projection of the essentially linear portion of the curves; for Arrangement A, this was an extrapolation of data from about 300 to 1500 ns back to zero, the time of the initial shock arrival at the gage. The extrapolation amounts to about 3% and the corresponding error is unlikely to exceed 1% of the particle velocity (see curves of Fig. 6). Table 2 gives a listing of all of the initial particle velocities obtained in this work plus other pertinent data for each of the experiments reported.

Comparison of the initial particle velocities obtained in these experiments with the smoothed results reported by Liddiard and Price[21] are given in Table 3. The results agree best at 10 mm; at 20 mm we have a spread of about 3% in our three data points and the average is about 4% higher. At 25 mm we are about 3% higher. It should be noted that only one experiment was performed with the fast response system at 20 mm. The u-t curve, shown in Fig. 7, is flat out to 200 ns. The expected decay in velocity would be about 2% in this time interval. The observed particle velocity agrees very well with the value extrapolated from measurements of the slower system. This agreement supports the contention that the earlier arrangement used for recording was adequate to give good initial particle velocities for X ≥ 10 mm. On the average the agreement of the EMV method with free surface measurement method for initial particle velocity is about 2 to 4%, about equal to the expected accuracy of either method of measurement.

B. Particle Velocities at Shorter Run Distances

The free surface velocity measurements of Liddiard and Price were limited by the experimental method to run distances of 10 mm or greater.[21] The acceptable agreement of our results with theirs at 10 to 25 mm encouraged us to use the EMV method to obtain new data in the range $0 < X < 10$ mm. This would serve to demonstrate how well the EMV method works when the particle velocities and gradients in the u-t curves are high. The first close-in experiments were, unfortunately, performed before we recognized the importance of oscilloscope response and the effect of oscilloscope connections to the gage on response. The first data are presented here chiefly for the purpose of illustrating the problem of system response and how it affects the extrapolated observations. When it became apparent that the system needed improvement, one oscilloscope was eliminated from the recording system. Although this improved the response, it was not considered good enough so only two experiments were run with it. The remaining experiments were done after the fastest oscilloscope was acquired.

It is clear from a look at Fig. 12, which presents all of the extrapolations to initial particle velocity plotted against run distance, that the results become very sensitive to system rise time when the run distance to the gage is less than about 5 mm. Linear extrapolation of late time data to shock arrival time underestimates the initial particle velocity when the rise time is large and the run distance is short. It is clear enough from an examination of the experimental set-up and the hydrodynamics related to it why this must be so. For a spherical detonation wave in the HE there is strong rarefaction following the detonation front, the spherical Taylor wave. The very steep initial gradient in the flow will level off along any particle path as time progresses. At the interface with the PMMA the result will be a transmitted shock also followed by a steep gradient in particle velocity vs time. This gradient will diminish on any particle path in the PMMA. When X increases, the steep gradient disappears as rarefactions overtake the shock front and the decay in the Taylor wave becomes more linear. Therefore, at the larger values of X, linear extrapolation to shock arrival time will be sufficient to predict the initial particle velocity from data taken at fairly late times after shock arrival. Close to the HE linear extrapolation will give acceptable answers only when the rise time of the recording system is short. In an effort to obtain a better feel for the rise time requirements to record a wave having a sharp inflection, a simplified problem on response has been worked out in Appendix D. In this problem the wave consists of two straight lines with a sharp break from the line of steeper slope to the line of lesser slope. It is shown that unless the rise time of the instrument system is short enough, all evidence of the steeper slope is lost in the response curve.

Also plotted in Fig. 12 are initial particle velocities from the free surface measurements previously discussed and computed values obtained from 1-D calculations to be discussed later.

The more precise data from this work on the initial values of particle velocity vs run distance has been summarized in Fig. 13. Points are from Arrangement C for X < 10 mm and from Arrangement A for X equal to or greater than 10 mm. The values of u for X less than 1 to 2 mm may be in substantial error because of recording system response. The remaining points should be good. The initial particle velocity is seen to be nearly linear in distance for X > 5 mm.

C. Comparison with Computer Results

Another check of the EMV gage would be a determination of the accuracy of the particle velocity as a function of time and initial distance from the HE interface. Lacking other experimental data for this purpose, the recorded results have been compared with results obtained by numerical computation. The experiment was simulated by considering the problem of a spherical wave in the HE intercepting the PMMA on a curved surface at a radius from the center equal to the height of the tetryl donor. The particle velocity in PMMA was then followed as a function of distance and time. The maximum distance used for comparison was 10 mm. The length of the PMMA in the computation was 20 mm so that the flow at X = 10 mm would not be affected by the free surface for several μsec. A prior 2-D code run with the LSGT set-up[27] showed that the flow on the axis could be described by a 1-D computation for a distance up to 10 mm from the HE interface. Computation was carried out with the WONDY Lagrange code published by the Sandia Corporation[28,29] The input and other details for the calculation are given in Appendix C. The constants chosen for the calculations introduces a rise time in the output of about 225 ns, a delay comparable to the rise time of recording Arrangement A. Comparative u-t curves for four initial values of X are given in Fig. 14. It should be pointed out that the computer code does not simulate a reaction zone. Zero times for both experiment and computation are the times of initial shock arrival. Computed particle velocities are on the particle path. If one takes the zero time for the experimental curve as reference, the computed curves would probably have to be shifted to the right to compensate for the neglect of the reaction zone. This shift would then require a small change in the C-J pressure in the HE to obtain a better overall fit to the experimental data. Neglecting these refinements is unlikely to introduce an appreciable error in the slopes of the computed curves. It can be seen that the slopes and relative magnitudes of the curves for each value of X are in good agreement except for the curves for X = 2 mm. In this case the rise time of the experiment is less than the rise time of the computation In addition, the experiment at this distance is undoubtedly affected by the presence of the reaction zone in the HE. The higher particle

velocity observed in the experiment is, therefore, plausible and probably the more correct value. On the whole we believe that the comparison with the calculation leads to the conclusion that the EMV gage can measure particle velocity on a particle path with good accuracy.

D. Shock Pressure vs Distance in the Large Scale Gap Test

The EMV measurements of particle velocity provide an independent calibration of the LSGT peak pressure vs distance. Figure 15 shows the result obtained by using Eqs. (2) and (3) to define the pressure. For comparison the results of the previous calibration[20] have also been plotted. The calculated peak pressure from the calculation are also shown. It may be noted that the results of free surface velocity measurements and our results are in good agreement for $X \geq 10$ mm. The earlier work differs significantly from ours for $X < 10$ mm. The agreement of the EMV calibration with the calculation is somewhat better than with the result of the previous calibration. The reason for the differences can be explained. In the previous work[20] the initial pressure in the PMMA at $X = 0$ was computed from the detonation pressure in tetryl, 195 kbars, and the impedance of the HE and the PMMA giving a pressure of 155 kbars in the PMMA. A greater pressure should have resulted if the effects of the von Neumann spike and the reaction zone were taken into account. A smooth curve was drawn between this approximate interface pressure and the data for $X \geq 10$ mm without regard to the detailed hydrodynamics of the problem. Since most explosives detonate in the LSGT at PMMA pressures less than 80 kbars, the error in the calibration at $X < 10$ mm would not generally be of much practical importance.

The calculation was started at $X = 0$ with the same assumed pressure, 155 kbars as that used in the calibration and one that is certainly too low. The computed results are therefore shifted an undertermined amount from the real pressure distance curve. (The present experimental results indicate that the pressure of 155 kbars should appear at about 1.5 mm from the interface.) If either the free surface result of the 1-D result were fit to a point $X = 1.5$ mm, $P = 155$ kbars the agreement with the present EMV results would probably be improved. Although the present EMV results probably describe the LSGT calibration for $X < 10$ mm better than any previous calibration, a few more experiments would be useful before the calibration is officially changed. The resulting Hugoniot data for PMMA using the present data is listed in Table 4.

VI. DISCUSSION

The main interest of this study was the development of the experimental method. Consequently, the report has assumed that the explosive is absolutely reproducible. We know this is not the case. The large number of experiments (about 45 for u-t records, 10 for noise elimination) conducted to obtain the desired data would not be required in future work. The study has demonstrated that the EMV gage can be applied to the measurement of particle velocity vs time on a particle path with an estimated error of about 2% in the particle velocity provided the proper oscilloscope instrumentation is used. There is evidence in the results that relative values of particle velocity within a given record are somewhat better than the absolute values.

The major problems encountered in this work are: (a) noise in the record from the detonation of the explosive and (b) large response time in recording. For the present experiments on PMMA the noise was eliminated by the use of appropriate shielding and by employing magnetic fields of the order of 1000 gauss. The long response time is now believed to have been largely due to electrical circuit impedance mismatch between the oscilloscope and the gage. Impedance matching for fast response oscilloscopes is apparently a much more critical problem than for oscilloscopes with response times in the 100 ns range. After taking all known precautions to eliminate sources of degradation of electrical circuit response, it was possible to obtain an overall effective rise time for the entire recording system of about 20 to 30 ns (13 micron foil of length 5 mm) when the 2.4 ns rise time oscilloscope was employed. This is about the value predicted when corrections for time to accelerate the foil of the gage and time for the curved shock to envelop the base of the gage are taken into account. A sharp break in the slope of a u-t curve would probably be detected if it occurred 70 ns or more after the initial shock pulse.

The results reported for initial particle velocity in the shock wave in PMMA are believed to be reasonably accurate extrapolations in spite of the fact that the recorded data for distances from the HE-PMMA interface exceeding 4 mm was obtained with a system having inferior response. This conclusion is based on the observance of slow decay rates in the particle velocity (at $X \geq 10$ mm) and confirmed by spot checks with the higher frequency oscilloscope. Future work will be conducted with the better recording system. We can expect the resulting records to be much

more useful and the number of shots for a series to be considerably fewer than was required here.

As an example of the possibilities we can cite the result obtained from shot number 183, Fig. 10c. If we had a series of records of this quality for X in the range 0 to 10 mm, it would be possible to correlate the data to obtain information about the sound speed in PMMA as a function of pressure. The more extensive data would, in addition be useful for tracking down the reason for the observed inflections in the recorded particle velocity time curves. It should be possible to relate the shape of the u-t curves to the shape of the peak particle velocity vs distance curve and, therefore, additional data at several values of X would help to determine more precisely the exact u_{max}-X relation. In view of the observation of breaks in the u-t curve on at least 3 records, we believe the behavior to be real. It has not been predicted in theoretical studies with or without the effect of reaction zone being considered. It therefore presents a challenging problem to be studied in more detail.

This work confirms the work of Dremin and his co-workers[7] concerning their ability to measure particle velocity in inert insulators by the magnetic method. It also gives us greater confidence in the work reported by the Russians on particle velocity in detonating explosives. What we have found out about effective rise times would indicate that experiments on detonating explosives with 100 micron foils have response rise times of the order of 75 ns. The time is determined chiefly by the foil thickness as long as the oscilloscope response is less than 7 ns or thereabout. With this response time it should be possible to detect a break in the u-t record occurring 75 ns or greater after the initial shock arrival in agreement with Dremin[7]. Experiments to measure particle velocity in a few explosives are now in progress here. The work will be reported later.

One of the main drawbacks of the EMV gage method is the requirement of a magnet of about 1000 gauss large enough to accommodate the experiment between the pole faces. We were limited to an experimental diameter of about 50 mm for the explosive charge because of the dimensions of the LSGT. Much larger diameters are desired for work in explosives, e.g., for measuring the ideal detonation pressure. Acquisition of a large magnet to permit experiments up to at least 80 mm diameter is strongly recommended.

Acknowledgment

This work was greatly aided by the suggestions from Donna Price. The assistance of Carl Groves and Leon Markulis in carrying out the experimental program is gratefully noted. We are also grateful to William Isbell of General Motors Materials and Structural Laboratory for suggesting the type of oscilloscope most suitable for our work and for suggesting diagnostic techniques and to E. H. Jackson for helping us with the diagnostics. Finally, we wish to thank D. J. Garrison of Tektronix, Inc. for suggestions for improving signal transmission.

REFERENCES

1. V. M. Zaitzev, P. F. Pokhil, and K. K. Shvedov, "The Electromagnetic Method for the Measurement of Velocities of Detonation Products", Doklady Acad. Sci. USSR, 132, 6, 1339 (1960).

2. A. N. Dremin and P. F. Pokhil, "Investigation of the Reaction Zone of TNT", Zh. Fiz. Chimia., 34, 11 (1960).

3. A. N. Dremin and Karpukhim. "Shock Adiabats of Paraffin", PMTF, No. 3, (1960).

4. S. T. Frazier, "Hypervelocity Impact Studies in Wax", BRL Rept. No. 1124 (Feb. 1961).

5. A. N. Dremin, V. M. Zaitzev, V. S. Ilyukhin, and P. F. Pokhil, "Detonation Parameters", 8th Symp. on Comb., Williams and Wilkins Co., Balti., p 610-619 (1962).

6. E. A. Ripperger and L. M. Yeakley, "Measurement of Particle Velocities Associated with Waves Propagating in Bars", paper presented at Annual Mtg of ASME, N. Y. (Nov. 1964).

7. A. N. Dremin and K. K. Shvedov, "The Determination of the Chapman-Jouguet Pressure and of the Duration of Reaction in the Detonation Wave of High Explosives", J. of Appl. Mech. and Tech. Phys., No. 2, p 154-159 (1964).

8. E. G. Johnson, "An Electromagnetic Technique for Measuring Particle Velocity in Shock Waves", Rohm and Haas Tech. Rept. S-181. (Feb. 1969).

9. J. T. Frasier and B. G. Karpov, "The Transient Response of Wax Target Subjected to Hypervelocity Impacts", Exper. Mech. 305-312 (Sep. 1965).

10. V. A. Veretennikov, A. N. Dremin and K. K. Shvedov, "Determination of the Detonation Parameters of Condensed Explosives", Comb., Explosion and Shock Waves, 1, 3, 1-5 (1965).

11. A. N. Dremin, S. V. Pershin, and V. F. Pogorelov, "Structure of Shock Waves in KCl and KBr. Under Dynamic Compression to 200,000 Atm.", Comb., Explosion and Shock Waves, 1, 4, 1-4 (1965).

12. A. N. Dremin, "Critical Phenomena in the Detonation of Liquid Explosives", 12th Symp. on Comb., Poitiers, France, 691-699 (1969).

13. L. G. Bokhovitinov, V. A. Vasiljev, and V. N. Rodinov, "Initiation of Detonation in Low Density TNT by Air Shock", 12th Symp. on Comb., Poitiers, France 771-777 (1969).

14. R. E. Duff and E. Houston, "Measurement of the Chapman-Jouguet Pressure and Reaction Zone Length in a Detonating High Explosive", J. Chem. Phys., 23, 7, 1268-1273 (1955).

15. W. E. Deal, "Measurement of Chapman-Jouguet Pressure for Explosives", J. Chem. Phys., 27, 3, 796-800 (1957).

16. F. J. Petrone, "Validity of the Classical Detonation Wave Structure for Condensed Explosives", The Phys. of Fluids, 11, 7, 1473-1478 (Jul. 1968).

17. B. G. Craig, "Measurement of the Detonation-Front Structure in Condensed-Phase Explosives", 10th Symp. on Comb., Cambridge, England, p 863-867 (Aug. 1964).

18. W. C. Davis, B. G. Craig, and J. B. Ramsay, "Failure of the Chapman-Jouguet Theory for Liquids and Solid Explosives", 4th Symp. on Det., p 84-85 (1965).

19. S. J. Jacobs, "The Electromagnetic Method for Particle Velocity Measurement in Shocks and Detonations", NOL Int. Memo.

20. D. Price and T. P. Liddiard, "The Small Scale Gap Test: Calibration and Comparison with the Large Scale Gap Test", NOLTR 66-87 (1966).

21. T. P. Liddiard and D. Price, "Recalibration of the Standard Card Gap Test", NOLTR 65-43 (1965).

22. G. E. Hauver, "Solid State Transducers for Recording of Intense Pressure Pulses", Ondes de Detonation, Editions du CNRS, 15 Quai Anatol France-Paris, p 363 (1962).

23. F. E. Allison, "Shock Induced Polarization in Plastics", J. Appl. Phys., 36, 2111 (1965).

24. G. E. Hauver, "Shock Induced Polarization in Plastics, II", J. Appl. Phys., 36, 2113 (1965).

25. R. H. Cole, "Underwater Explosions", Princeton Univ. Press, Princeton (1948), p. 200.

26. D. Price, I. Jaffe, and J. P. Toscano, "Development of the Continuous Wire Method, Progress Report II", NOLTR 66-21 (1966).

27. E. E. Fisher, R. G. Johnson, and R. F. Paulson, "Simulation of the Dynamical Loading of PMMA in the NOL Regular Card Test", NOLTR 69-219 (1969).

28. W. Herrmann, P. Holzhauser, and R. J. Thompson, "WONDY, A Computer Program for Calculating Problems of Motion in One Dimension", Sandia Corp. Res. Rept. 66-601 (Feb. 1967).

29. J. O. Erkman and D. J. Edwards, "Computer Code for Calculating One-Dimensional Flow", NOLTR 68-160 (1968).

TABLE 1

RISE-TIME ESTIMATES FOR VARIOUS SCOPE ARRANGEMENTS

ℓ (mm)	T_1 (ns)	T_2 (ns)	T_3 (ns)	T_0 (ns)	T_{max} (ns)	T_{lin} (ns)
			Arrangements A and B (H-P 160 Scope)			
10	32	9	25	42	63	85
5	8	9	25	33	50	66
			Arrangement C (Tek 454 Scope)			
10	32	9	2.4	33	50	66
5	8	9	2.4	11.5	17	23

T_0 system rise time

T_1 taken as 0.8 τ_C (Eq. (6)); $r_0 \sim 55$ mm, $U \sim 5.5$ mm/μsec

T_2 time for two double transits at 6 mm/μsec in a 0.013 mm foil

T_3 scope rise time (10 - 90%)

T_{max} taken as 1.5 T_0

T_{lin} taken as 2.0 T_0

TABLE 2

INITIAL PARTICLE VELOCITY AS A FUNCTION OF X FOR PMMA

Distance X (mm)	Shot No.	Length of Pickup (mm)	Magnetic Field (gauss)	Measured Particle Velocity (mm/μsec)
		System A		
0.25	46	10.0	1410	2.06
0.25	51	5.0	1250	2.01
0.9	49	5.0	1190	1.90
1.0	52	5.0	1225	1.90
1.5	54	5.0	1275	1.83
1.5	55	5.0	1230	1.84
2.0	56	5.0	1160	1.78
2.0	53	5.0	1275	1.77
2.7	43	10.0	1100	1.70
2.8	45	10.0	1455	1.71
4.4	40	10.0	1180	1.65
4.6	44	10.0	1250	1.63
6.9	42	10.0	1240	1.52
7.1	39	10.0	1300	1.53
10.0	41	10.0	1305	1.43
10.0	38	10.0	1255	1.42
20.0	24	10.0	535	1.11
20.0	25	10.0	920	1.15
25.0	27	5.0	980	1.03
25.0	28	5.0	980	1.01
		System B		
2.2	87	5.0	1200	1.89
4.8	88	5.0	1350	1.60
		System C		
0.25	118	5.0	770	2.26
0.25	120	5.0	700	2.27
0.85	108	10.0	980	2.25
0.86	183	5.0	779	2.22
2.0	119	5.0	748	2.05
3.0	117	5.0	790	1.88
4.0	116	5.0	790	1.61
20.0	121	5.0	725	1.14

TABLE 3

COMPARISON OF THE EMV AND FREE SURFACE RESULTS

Shot No.	Gap Length, X (mm)	Magnetic Field (gauss)	Free Surface* Velocity (mm/μsec)	Particle** Velocity (mm/μsec)	EMV Particle Velocity (mm/μsec)
38	10	1355	2.84	1.42	1.42
41	10	1305	2.84	1.42	1.43
24	20	535	2.174	1.09	1.11
25	20	920	2.174	1.09	1.15
121	20	725	2.174	1.09	1.14
27B	25	980	1.98	0.99	1.03
28	25	980	1.98	0.99	1.01

* Table 4, reference (21)

** $u = 0.5\ u_{fs}$

TABLE 4

HUGONIOT DATA FOR PMMA

Gap Lenghth, X (mm)	Peak Particle Velocity (mm/μsec)	Shock Velocity (mm/μsec)	Peak Pressure (Kbar)
0.25	2.27	6.22	166.6
0.86	2.25	6.19	164.3
2.0	2.05	5.87	142.0
3.0	1.88	5.60	124.2
4.0	1.61	5.16	98.1
4.8	1.60	5.15	97.2
6.9	1.52	5.02	90.0
7.1	1.53	5.03	90.8
9.9	1.43	4.87	82.2
10.0	1.42	4.86	81.4
20.0	1.14	4.41	59.3
25.0	1.02	4.21	50.7

NOLTR 70-79

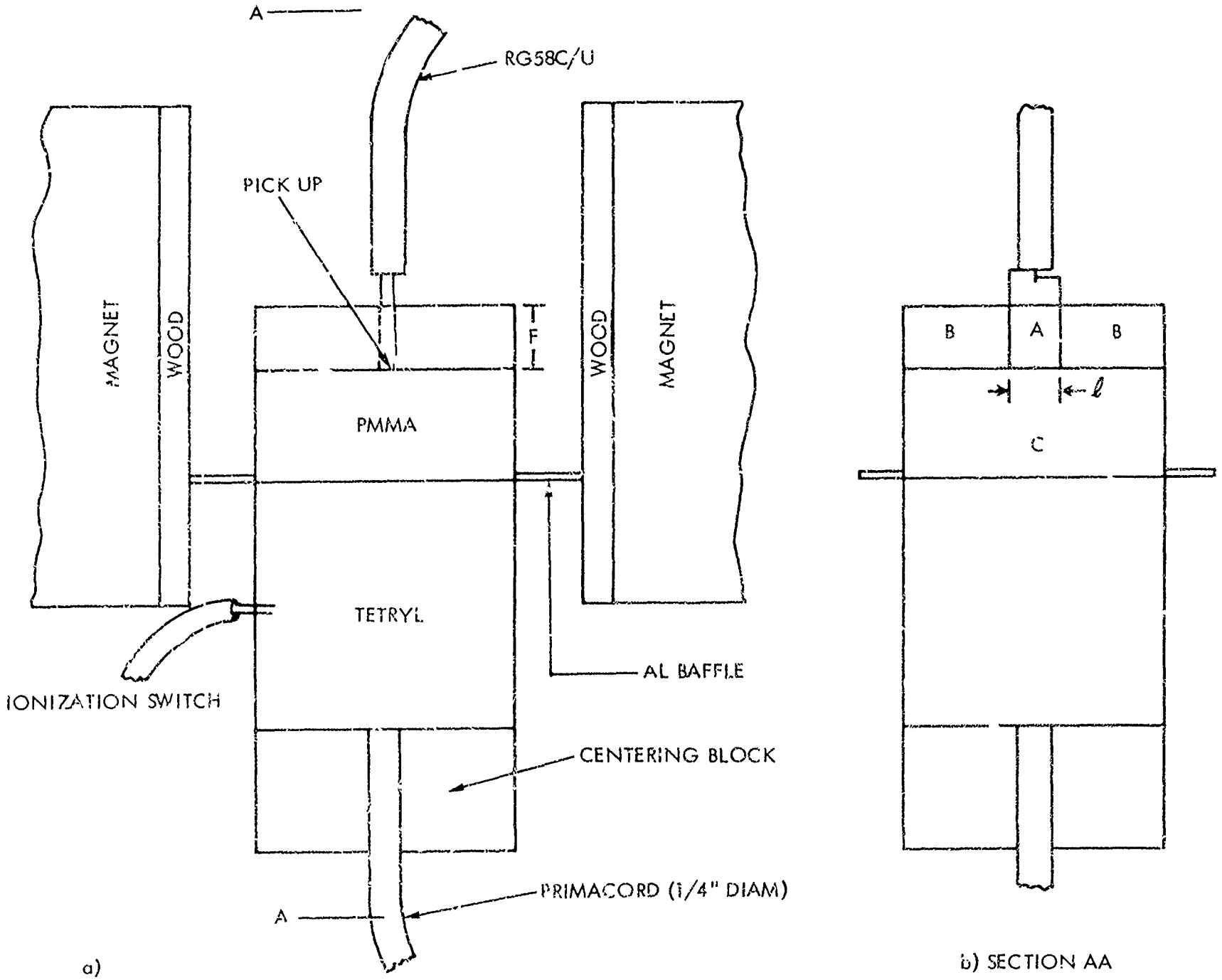

FIG. 1 EXPERIMENTAL SETUP

NOLTR 70 - 79

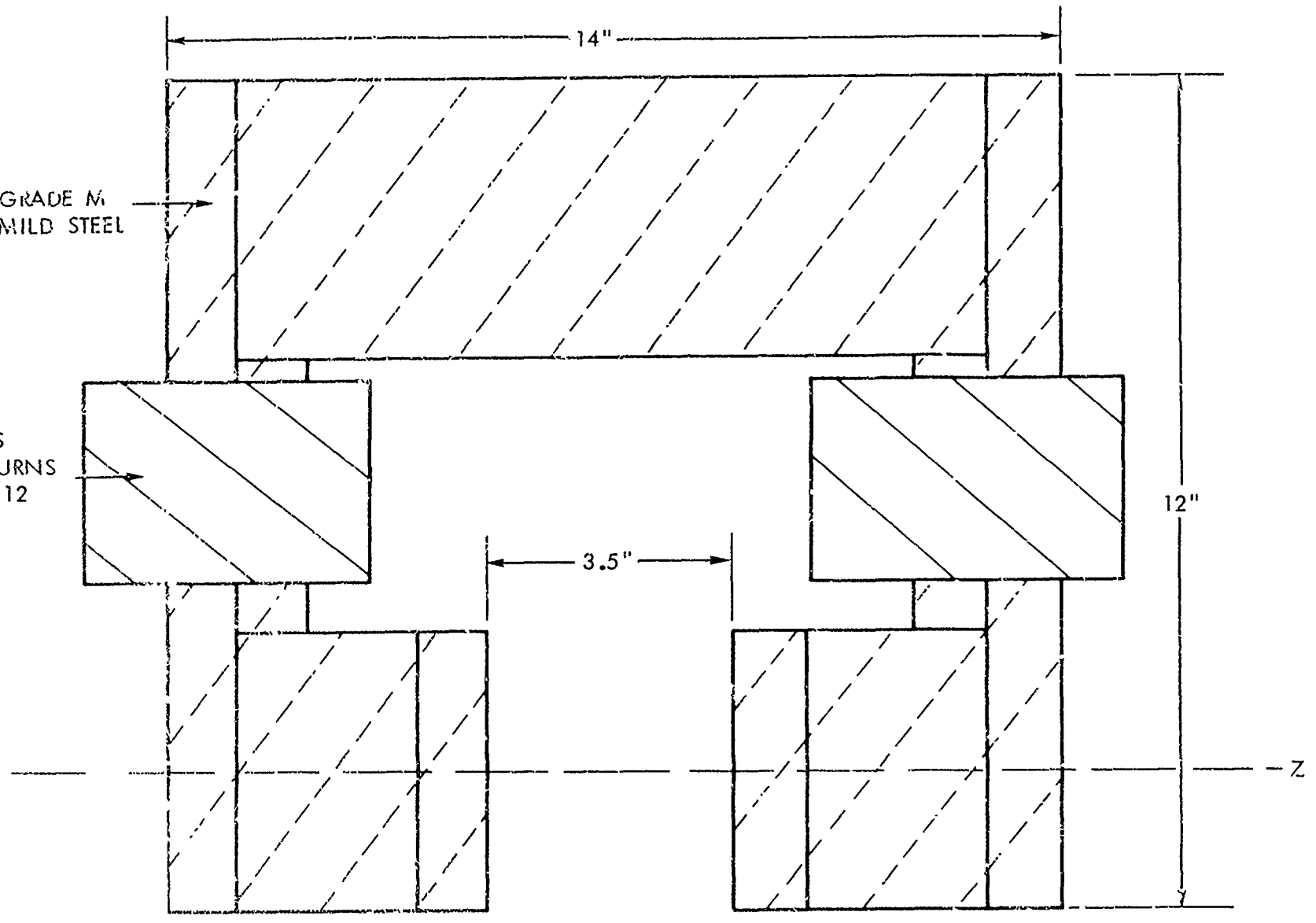

NOLR 70 - 79

SCALE 1 : 2

FIG. 2 DESIGN OF ELECTROMAGNET USED

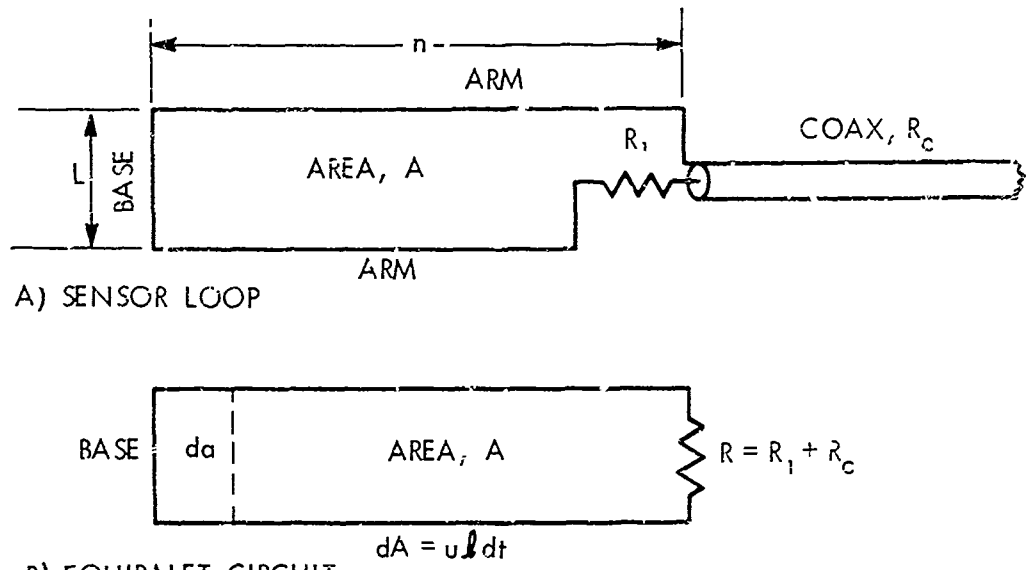

FIG 3 EMV GAGE CIRCUIT DIAGRAM

ρ_oU: PMMA,5
AL, 14

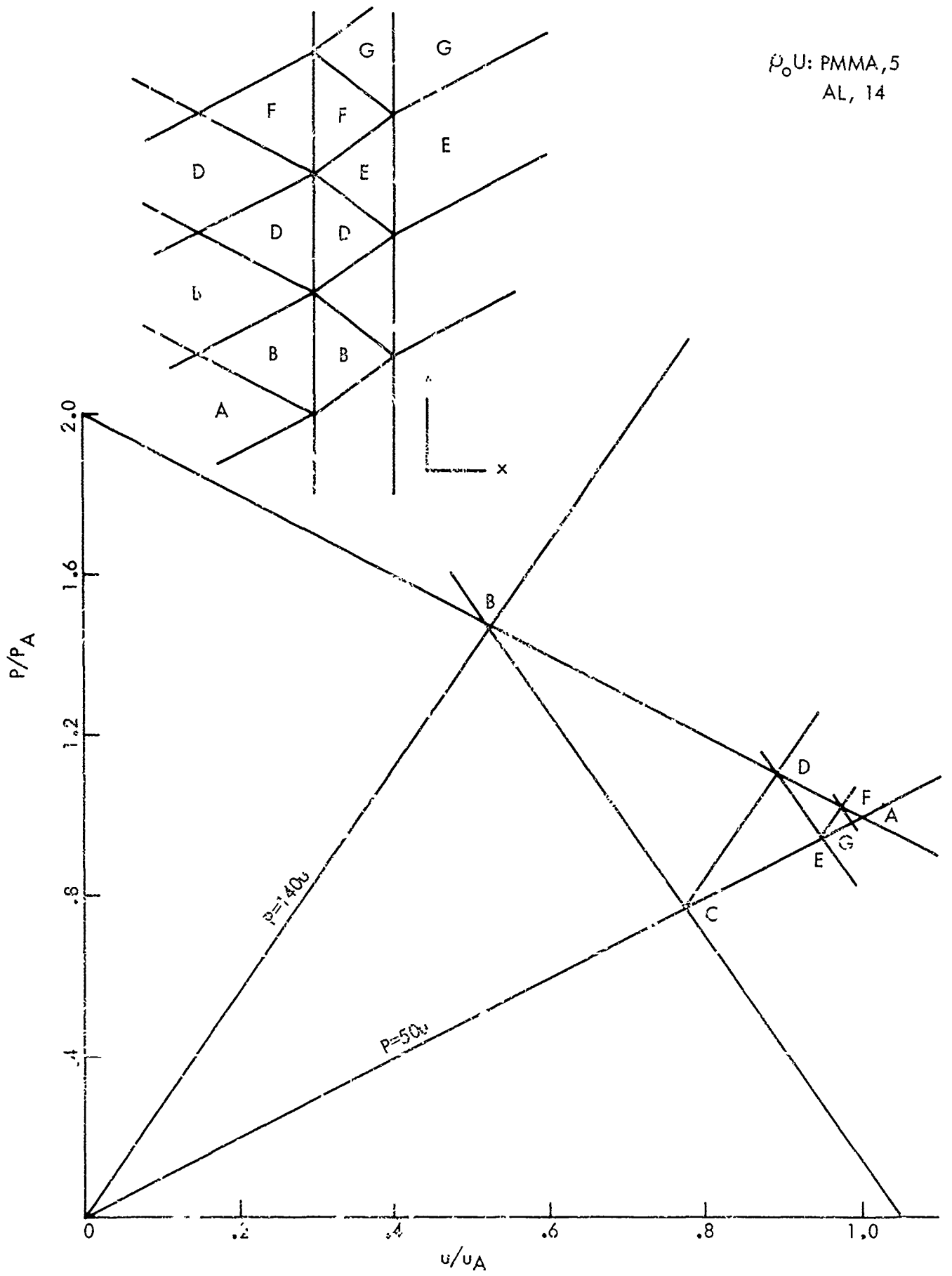

FIG. 4 LINEARIZED APPOXIMATION FOR PMMA-AL FOIL-PMMA

A. GAGE AT X 19mm
NO BAFFLE PRESENT
TIME MARKS: 1 μ SEC
PEAK TO PEAK

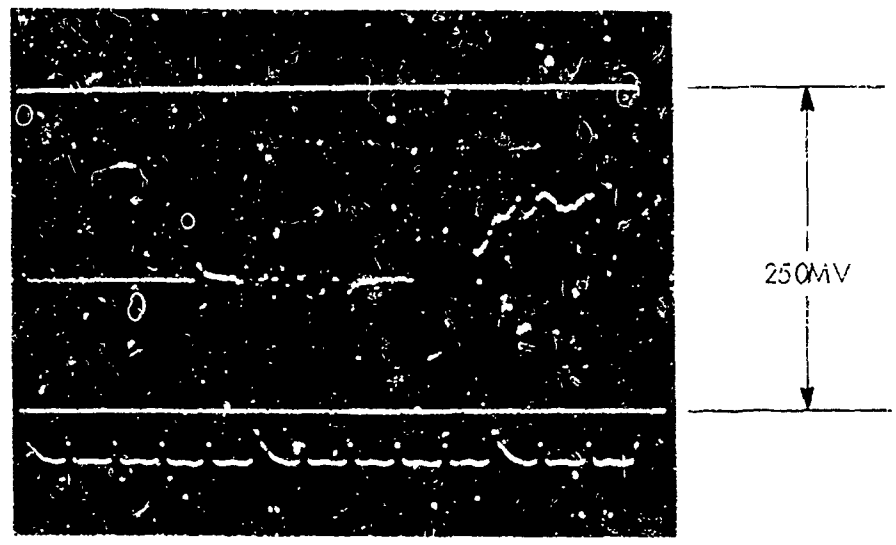

B. GAGE AT X 19mm
GROUNDED AL COLLAR BAFFLE
TIME MARKS: 1 μ SEC
PEAK TO PEAK

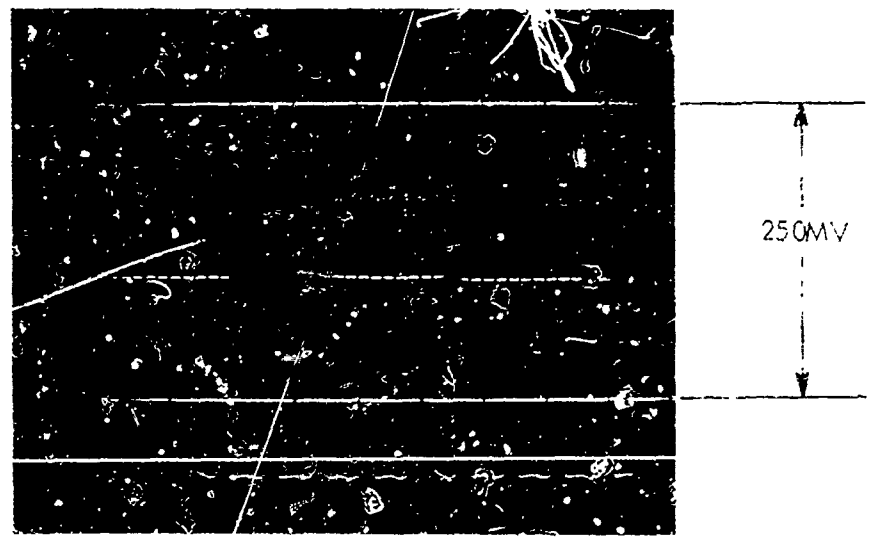

FIG. 5 ZERO FIELD RECORDS

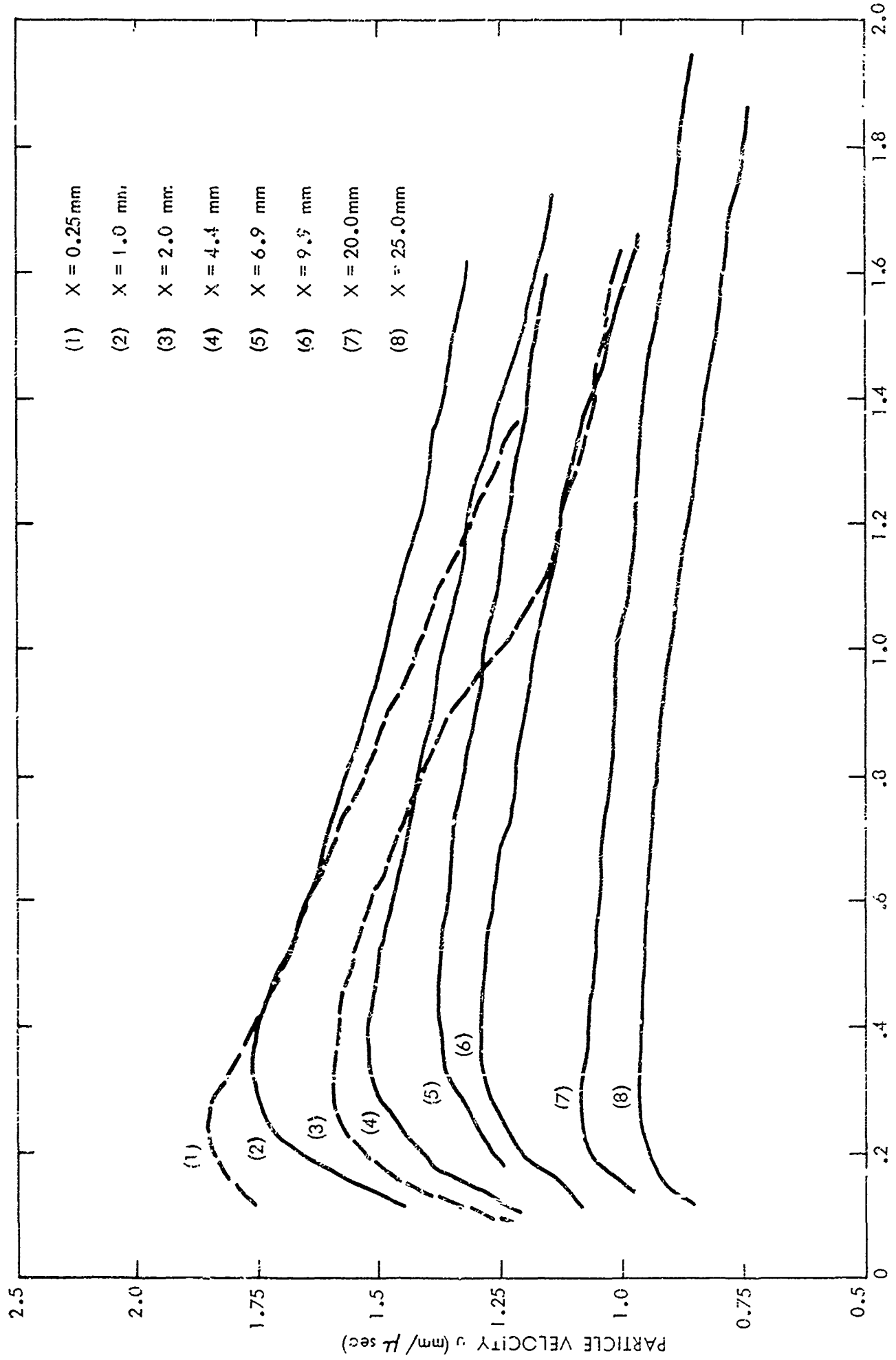

FIGURE 6 v-t CURVES OBTAINED USING ARRANGEMENT A

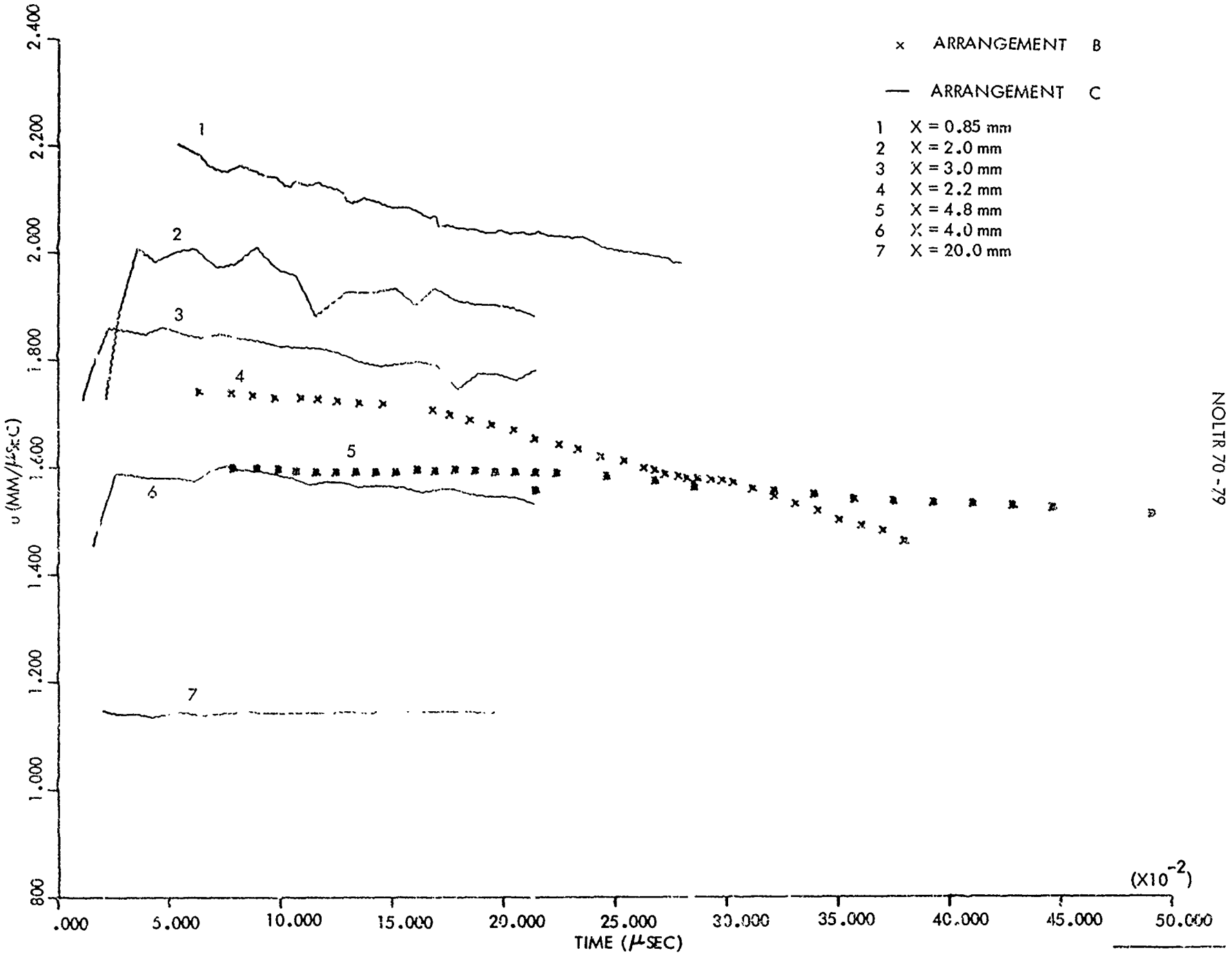

FIG. 7 u - T CURVES OBTAINED USING ARRANGEMENTS B AND C

ARRANGEMENT A

SHOT # 44
GAGE AT X = 4.6
FIELD: 1250 GAUSS

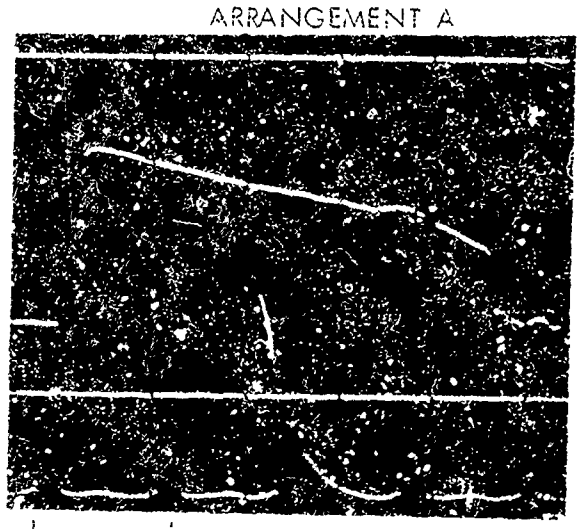

4 VOLTS

1 μ SEC

ARRANGEMENT B

SHOT # 88
GAGE AT X = 4.8mm
FIELD: 1350 GAUSS

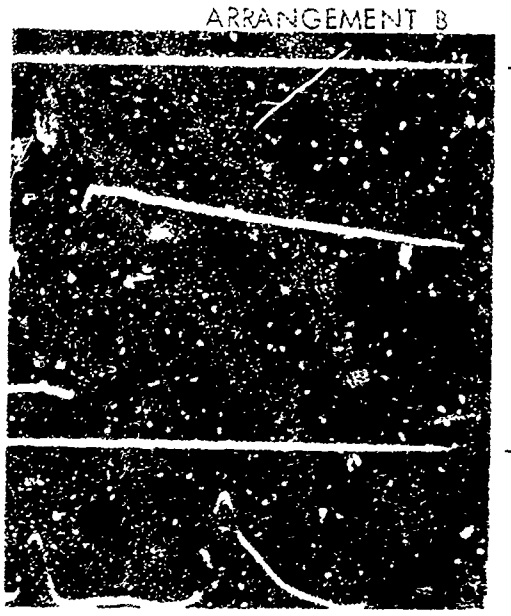

2 VOLTS

1 μ SEC

ARRANGEMENT C

SHOT # 108
GAGE AT X = 0.86mm
FIELD: 980 GAUSS

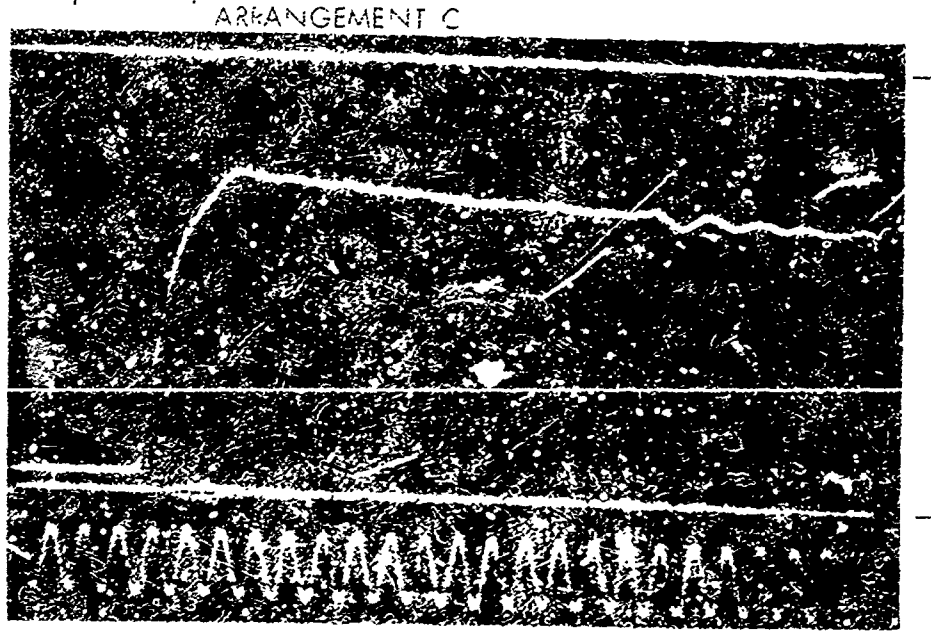

1.5 VOLTS

FIG. 6 TYPICAL RECORDS

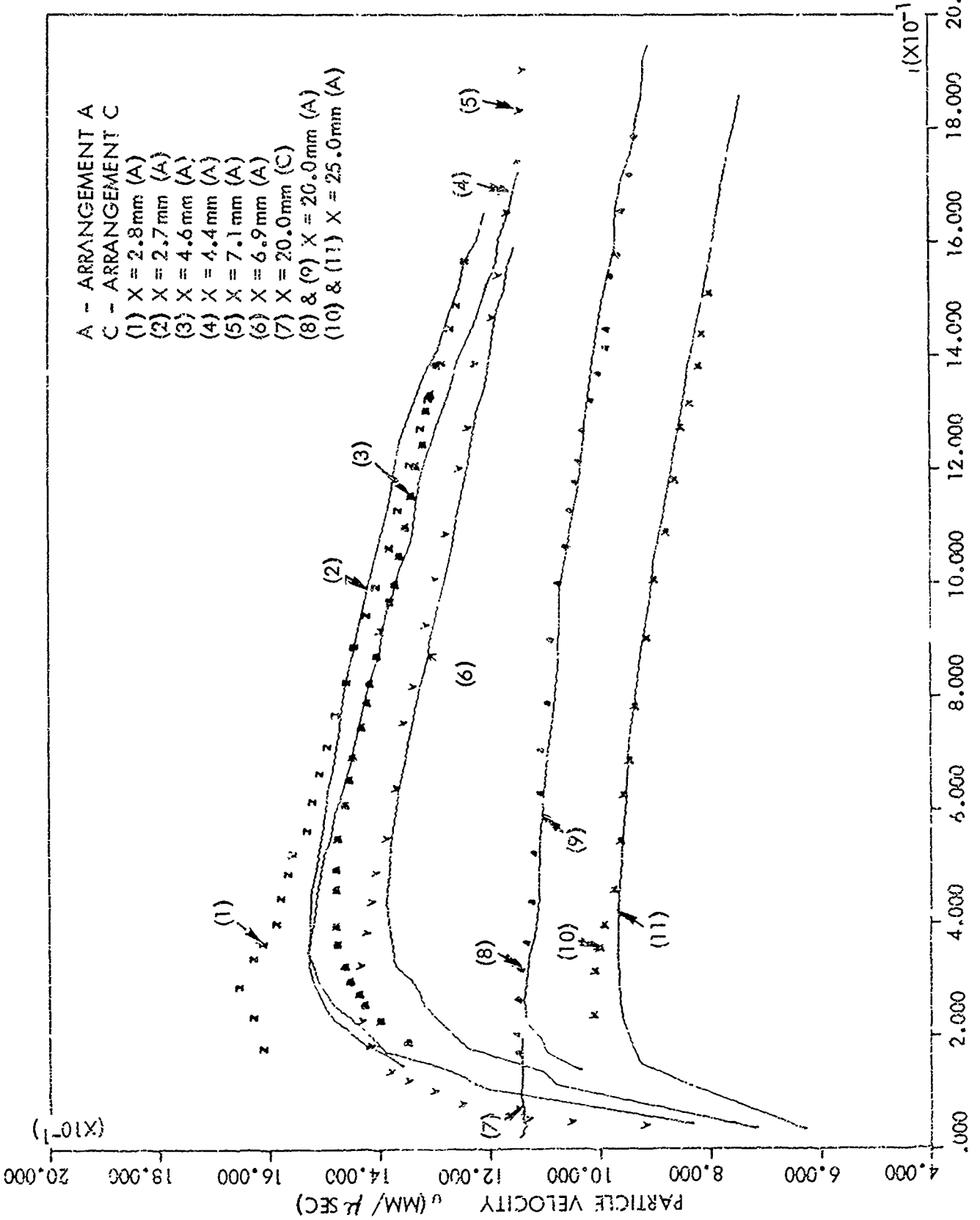

FIG. 9 REPRODUCIBILITY OF PMMA DATA

A
SHOT # 92
FIELD 1020 GAUSS

B
SHOT # 97
FIELD 982 GAUSS

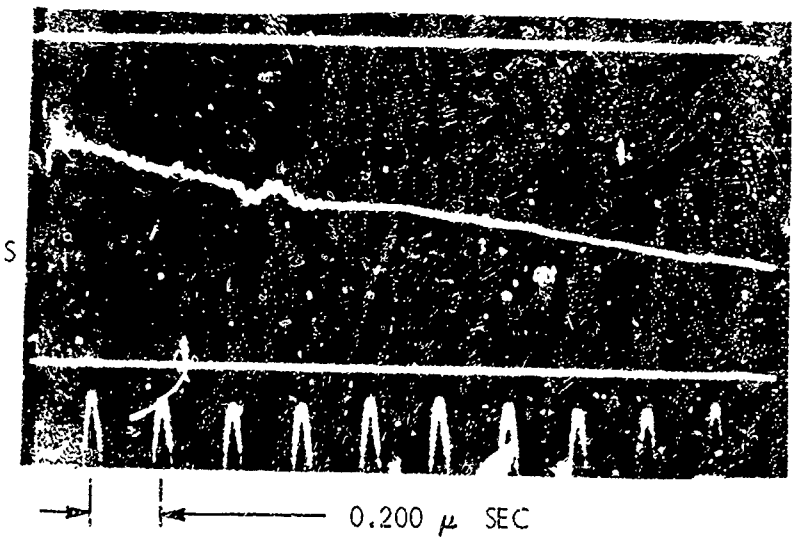

C
SHOT # 183
FIELD 779 GAUSS

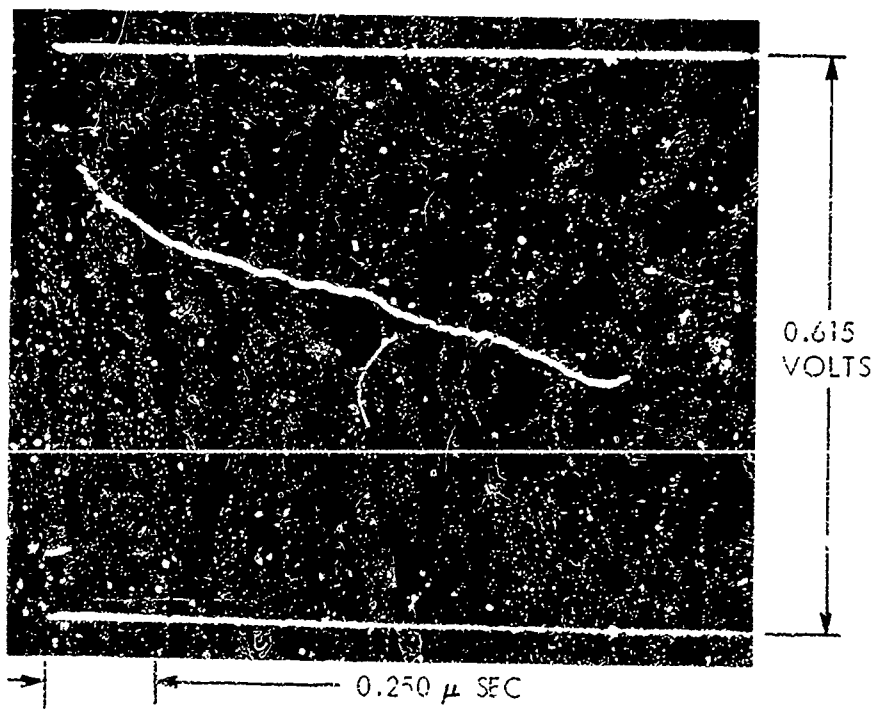

FIG. 10 RECORDS FOR X = 0.86mm

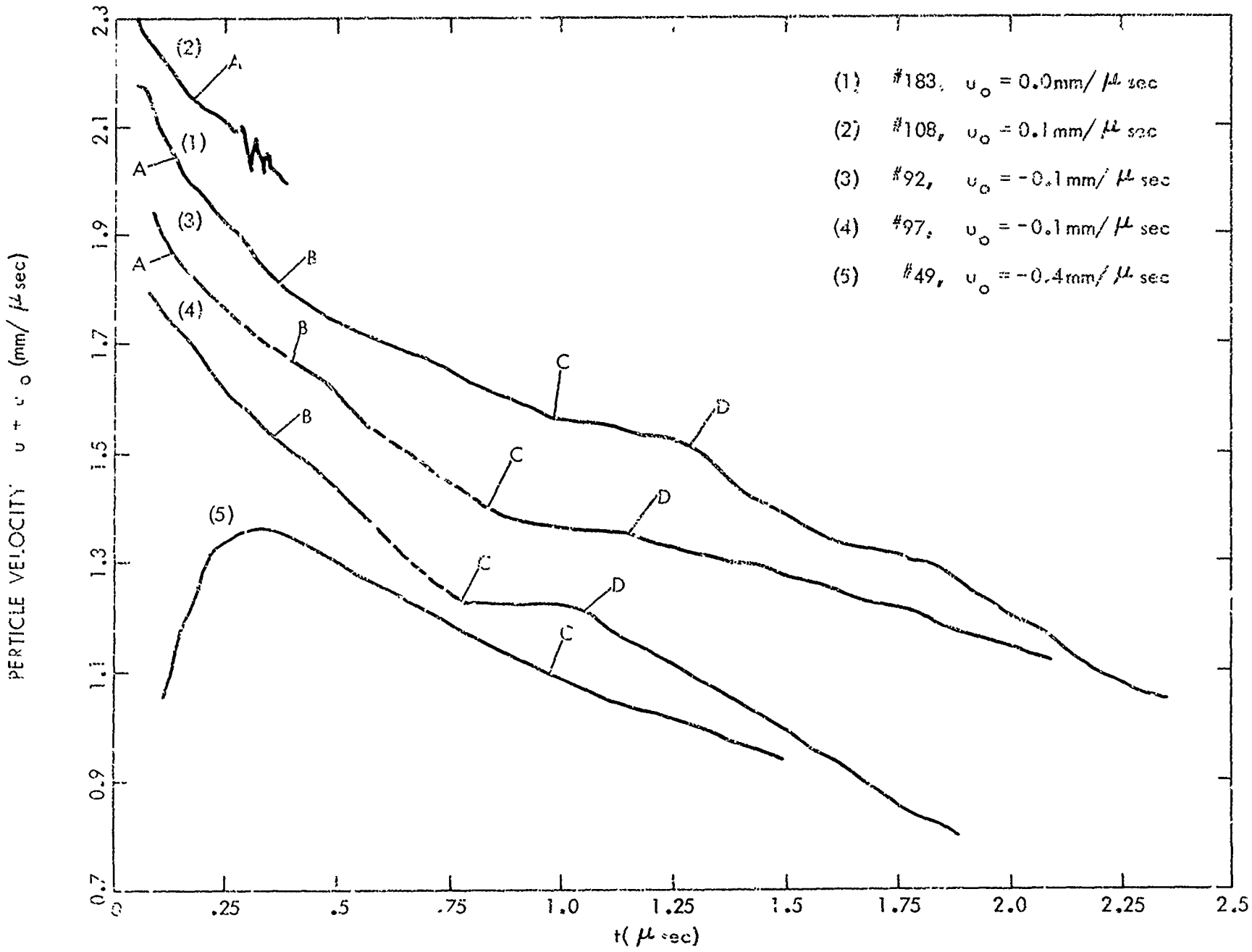

FIG. 11 u, t RECORDS FOR X = 0.86 mm

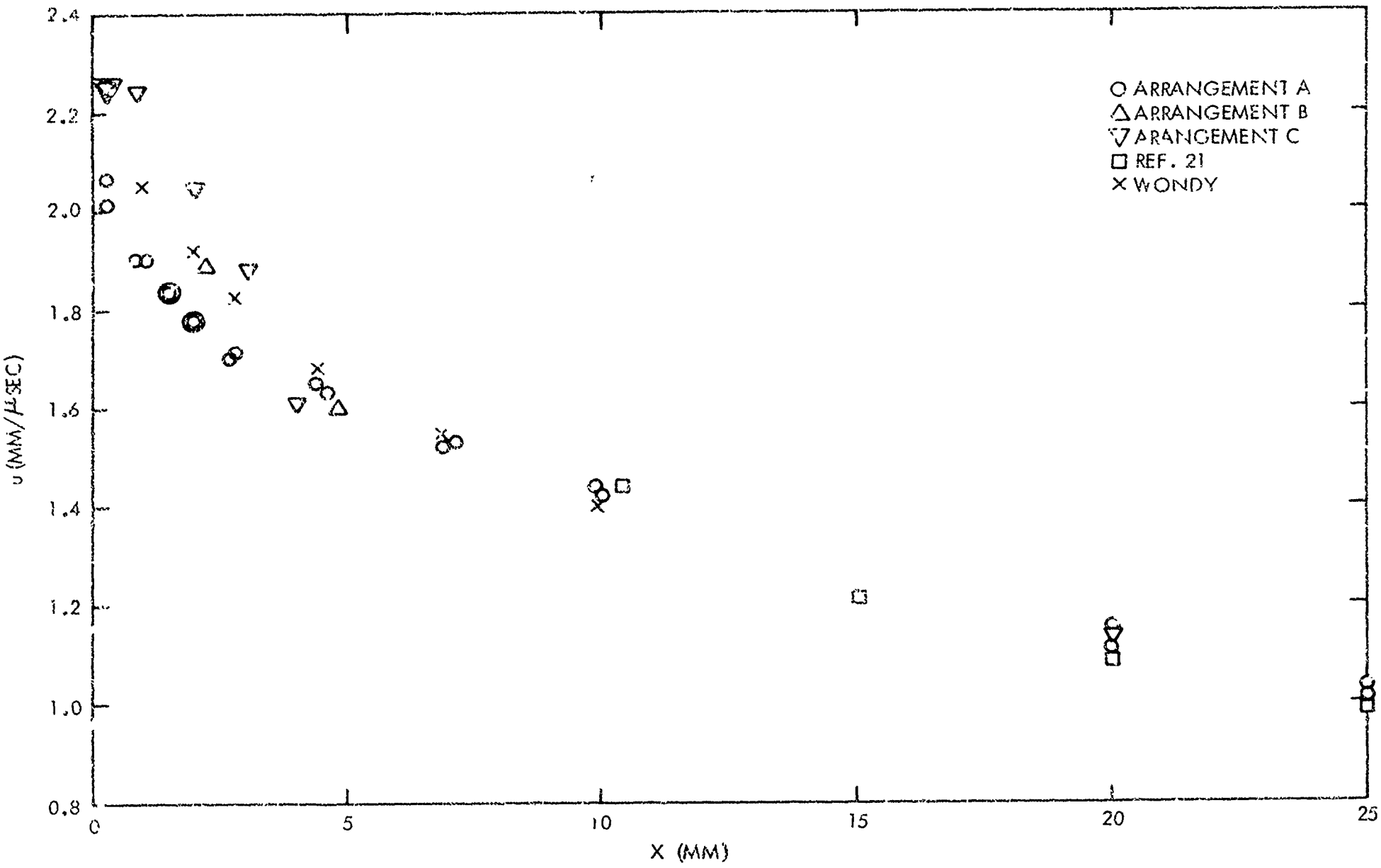

NCLTR 70 - 79

FIG. 12 PEAK PARTICLE VELOCITY VS DISTANCE FROM HE-PMMA INTERFACE (ALL DATA)

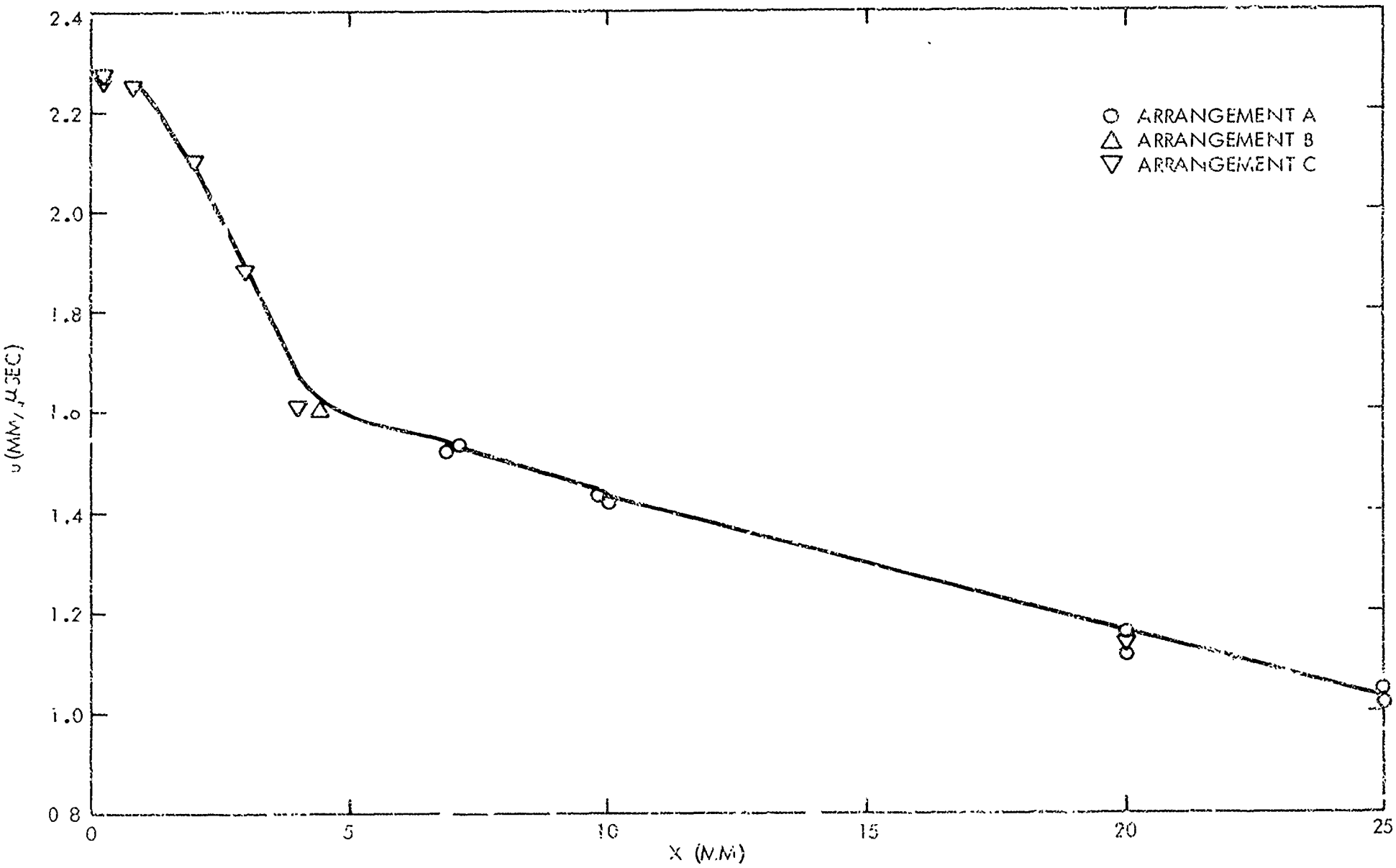

NOLTR 70 - 79

FIG. 13 EXTRAPOLATED PEAK PARTICLE VELOCITY VS DISTANCE FROM HE-PMM A INTERFACE (SELECTED DATA)

FIG. 14 COMPARISON OF EMV RESULTS WITH WONDY RESULTS

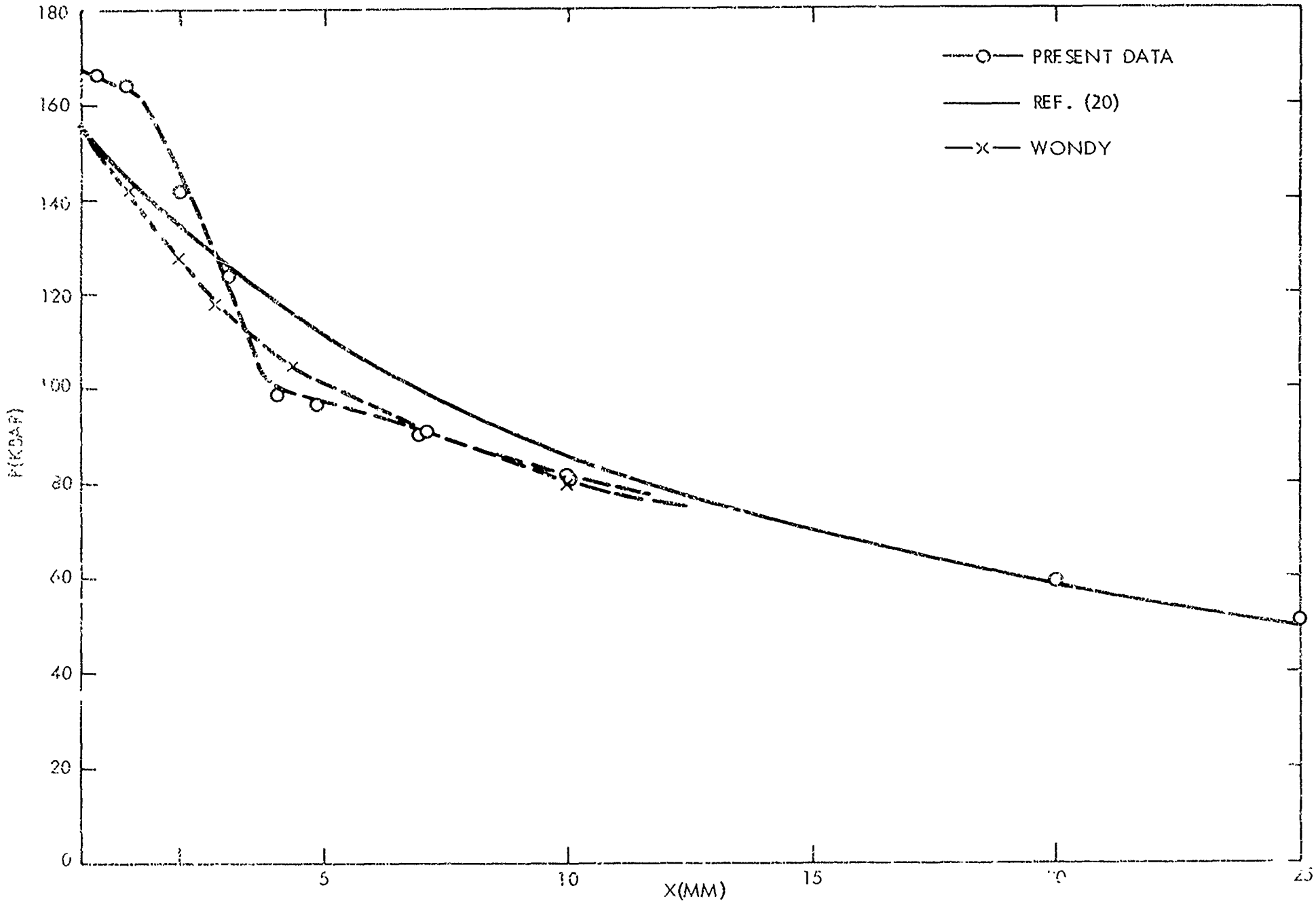

NOLR 70-75

FIG. 15 PEAK PRESSURE VS DISTANCE FROM
HE - PMMA INTERFACE

APPENDIX A

RESPONSE OF A SIMPLE RC CIRCUIT TO A TRIANGULAR INPUT PULSE

A simple RC circuit consisting of a resistance and capacitance in series with the input voltage $e_0(t)$ connected across the entire circuit and the output $e(t)$ across the capacitor serves as a good approximation for the analysis of the high frequency response of an oscilloscope and its connected circuitry, Fig. A-1. For comparison with the EMV gage it is of interest to compute the response of this circuit when the input e_0 is a jump to e_{00} followed by a linear decay, that is

$$e_0 = e_{00}(1 - at) \quad . \tag{A-1}$$

Ohm's law gives the current $i(t)$ for this circuit as

$$e_0 = iR + \frac{1}{C}\int i\,dt \tag{A-2}$$

and the response voltage as

$$e = e_0 - iR \quad . \tag{A-3}$$

The initial condition, when the voltage has jumped to e_{00}, is $i_{00} = e_{00}/R$, $t = 0$. By combining Eq. (A-2) with Eq. (A-1) and differentiating, one obtains

$$-dt = R\,di/(e_{00}\,a + i/C) \quad . \tag{A-4}$$

Integration then leads to

$$-t/\tau = \ln(e_{00}aC + i) + \ln(\text{const}) \tag{A-5}$$

in which $\tau = RC$. The solution can be written in the form

$$e_{00}aC + i = A\exp(-t/\tau) \quad . \tag{A-6}$$

Introducing the initial conditions defines the constant, A as

$$A = e_{00}(aC + 1/R) \quad .$$

Using Eq. (A-3) we then obtain

$$e = e_{00}[1 - at - (a\tau + 1)\exp(-t/\tau) + a\tau] \quad . \quad (A-7)$$

When τ goes to zero Eq. (A-7) reduces to the input voltage given by Eq. (A-1). When a is zero the input is a step jump and the response is

$$e/e_{00} = 1 - \exp(-t/\tau) \quad (A-8)$$

the response to a square step. It is apparent that the departure of the response, Eq. (A-7), from the input, Eq. (A-1), depends on both a and τ. The behavior of Eq. (A-7) can be illustrated in dimensionless variables by choosing a dimensionless time $\theta = t/\tau$. This gives the dimensionless voltage as

$$e/e_{00} = 1 - a\tau\theta - (a\tau + 1)\exp(-\theta) + a\tau \quad . \quad (A-9)$$

Solutions of Eq. (A-9) have been plotted in Fig. A-2 together with the corresponding input functions now given as

$$e_0/e_{00} = 1 - a\tau\theta \quad . \quad (A-10)$$

In the case of the step jump (a = 0) it is seen that the point of 90% response occurs at 2.30 τ. We note that the time to 10% response is 0.1 τ. We can therefore say for the simple RC network that the rise time $T_0 = 2.20\ \tau$. In the case of triangular input the departure of the maximum response from the input function increases as the value of $a\tau$ increases. The dimensionless time to maximum decreases as the value of $a\tau$ increases. It is of the order of magnitude of 3 τ or 1.5 T_0. T_{lin} is independent of slope and has a value of about 4.5 τ or 2 T_0.

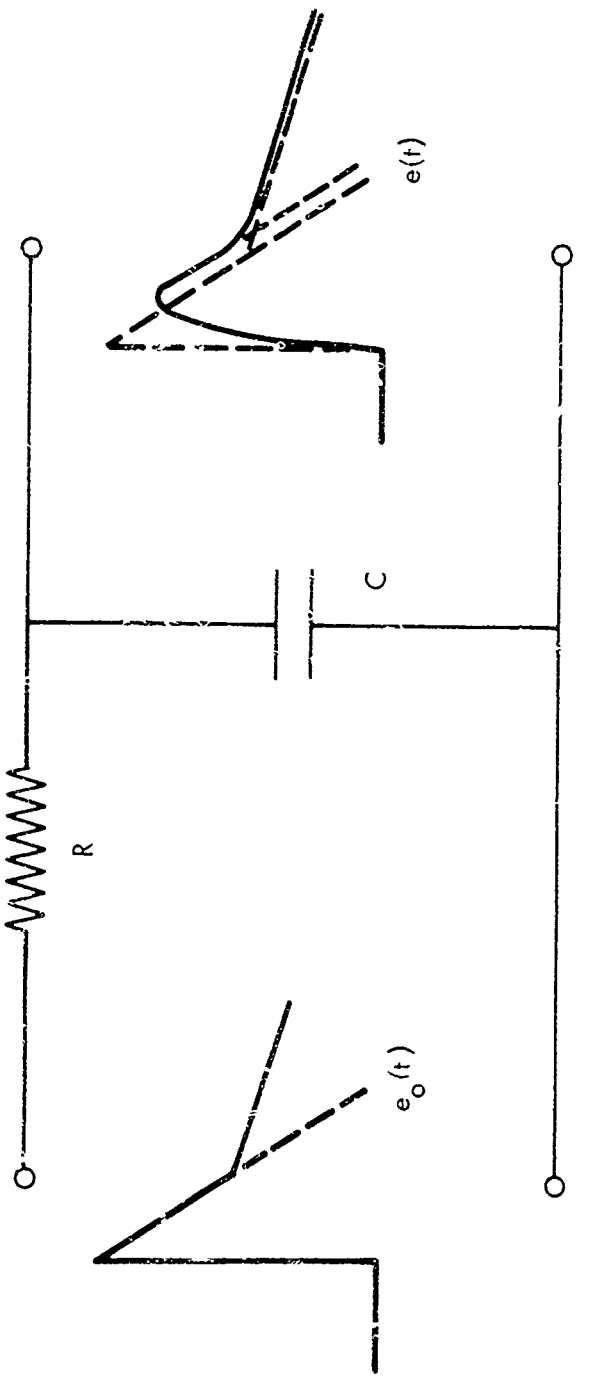

FIG. A-1 RC CIRCUIT

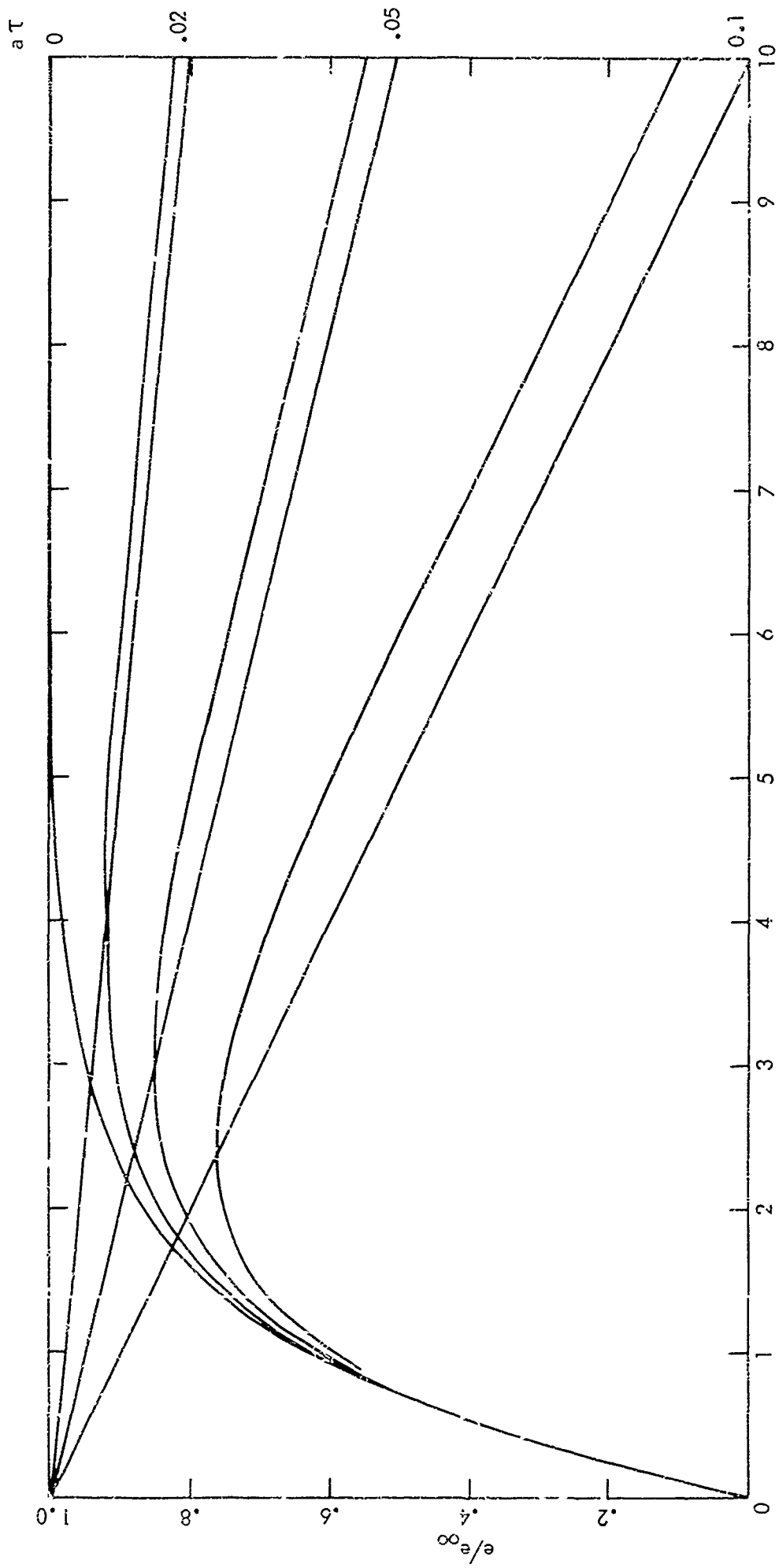

FIG. A-2 RESPONCE TO TRIANGULAR INPUT

APPENDIX B

RESPONSE OF TWO SIMPLE RC CIRCUITS IN SERIES TO A STEP FUNCTION

The response of a simple RC network to a step jump input has been derived as a special case in Appendix A, Eq. (A-8). If this function is used as the input to a second RC network as in Fig. A-1, the output $e_1(t)$ will be the response of two similar networks in series to a step input. In the text an approximate formula was given for the rise time of several RC networks in series. The purpose of this exact analysis for two networks is to see how well the approximation works for a case where the output can be exactly defined. The rise time for the exact case will be defined as previously; the time from 10 to 90% response.

Except for change in subscript the integral equation is as before, Eq. (A-8),

$$e_1 = Ri + \frac{1}{C}\int i\,dt \quad ; \tag{B-1}$$

e_1 being the voltage e of Eq. (A-8). Substituting for e_1 into Eq. (B-1) and differentiating gives

$$de_1/dt = (e_{oo}/\tau_1)\exp(-t/\tau_1) = R\,di/dt + i/C \tag{B-2}$$

where τ_1 is used to define the time constant of the input function. Using τ_2 to define the time constant RC of the second circuit, we can write

$$di/dt + i/\tau_2 = (e_{oo}/R\tau_1)\exp(-t/\tau_1) \quad . \tag{B-3}$$

This equation is of the form $di/dt + iP(t) = Q(t)$. It can be solved by forming the integral $I = \int P\,dt$. The solution, found in elementary texts on differential equations is then

$$i\exp(I) = \int QI\,dt + \text{const} \quad . \tag{B-4}$$

The integration for Eq. (B-3) turns out to give

$$i = \frac{e_{oo}\tau_2}{R(\tau_2 - \tau_1)}\exp(-t/\tau_1) + A\exp(-t/\tau_2) \quad . \tag{B-5}$$

When $t = 0$, $i = 0$ and therefore

$$A = (\tau_2 \, e_{oo}/R)/(\tau_2 - \tau_1) \quad . \tag{B-6}$$

The final solution for $e/e_{oo} = e_1/e_{oo} - Ri$ is then

$$e/e_{oo} = 1 - \exp(-t/\tau) - \frac{\tau_2}{\tau_1 - \tau_2} \left[\exp(-t/\tau_1) - \exp(-t/\tau_2) \right] \quad . \tag{B-7}$$

Equation (B-7) is indeterminate for $\tau_1 = \tau_2$. In this particular case the solution can be obtained by a limiting process. It becomes for $\tau_1 = \tau_2 = \tau$

$$e/e_{oo} = 1 - (1 + t/\tau) \exp(-t/\tau) \quad . \tag{B-8}$$

Equation (B-8) is compared with the result for a single network, all time constants being equal, in Fig. B-1. For this case the time to 90% response is 3.9 τ. It is seen that for the two networks in series the time to 10% response is fairly large. In this special case it is about 0.5 τ. The rise time for the series networks is therefore about 1.53 times the rise time for a single network. Equation (7) predicts 1.41 as the ratio. Times to 10% and 90% response have been computed for various ratios of τ_2/τ_1. Figure B-2 presents these data in the dimensionless variables T_o/T_{1o} versus the corresponding time constant ratio. In this plot the rise time T_o has been corrected to include the time to 10% response. Also plotted is the result from Eq. (7). Equation (7), although not exact, is nevertheless seen to be sufficiently accurate for its intended purpose. Note that the results plotted from 0 to 1 in the time constant ratio are sufficient to cover all possible combinations of time constants inasmuch as the larger of two time constants can always be taken as τ_1.

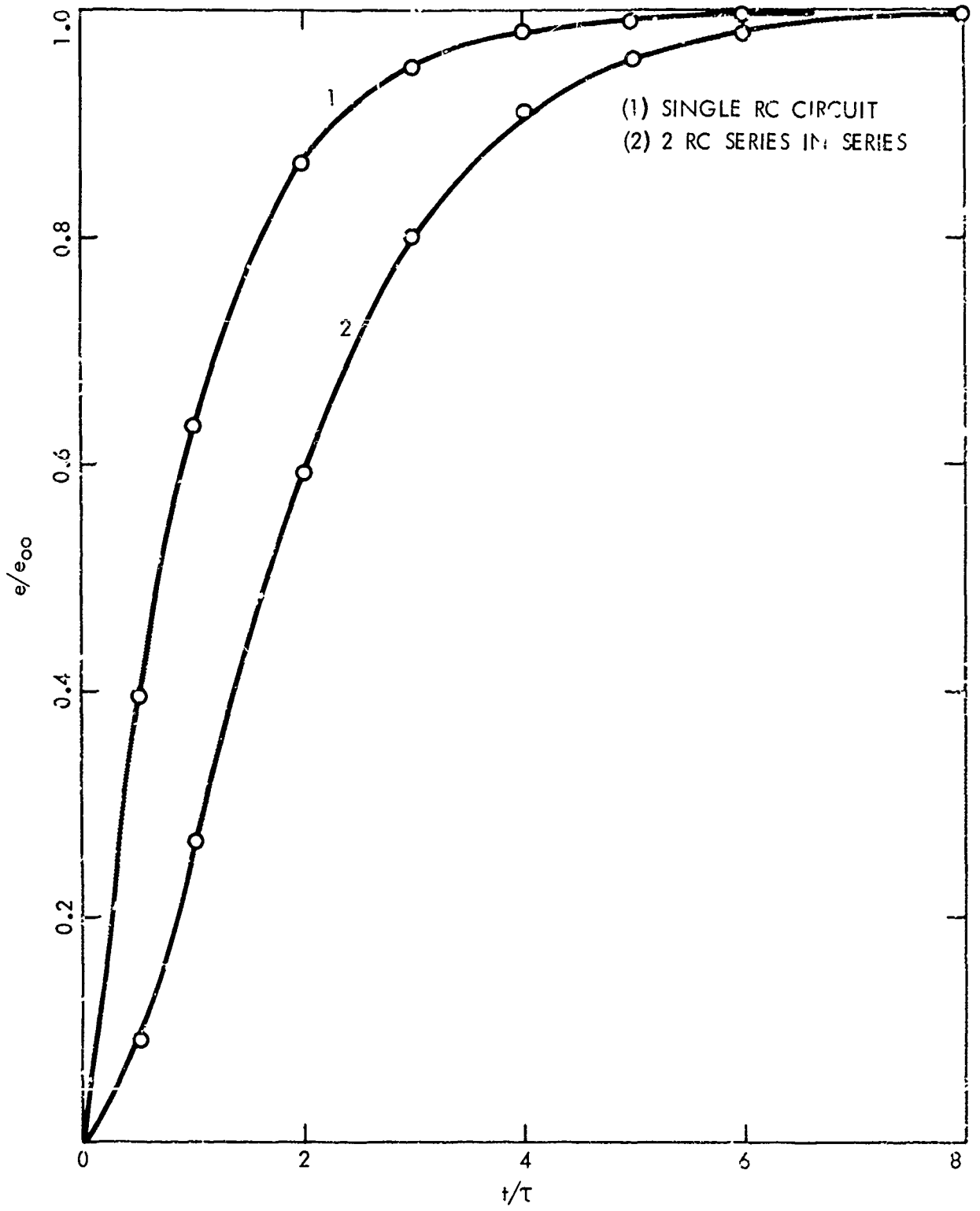

FIG. 8-1 RESPONSE TO A STEP INPUT

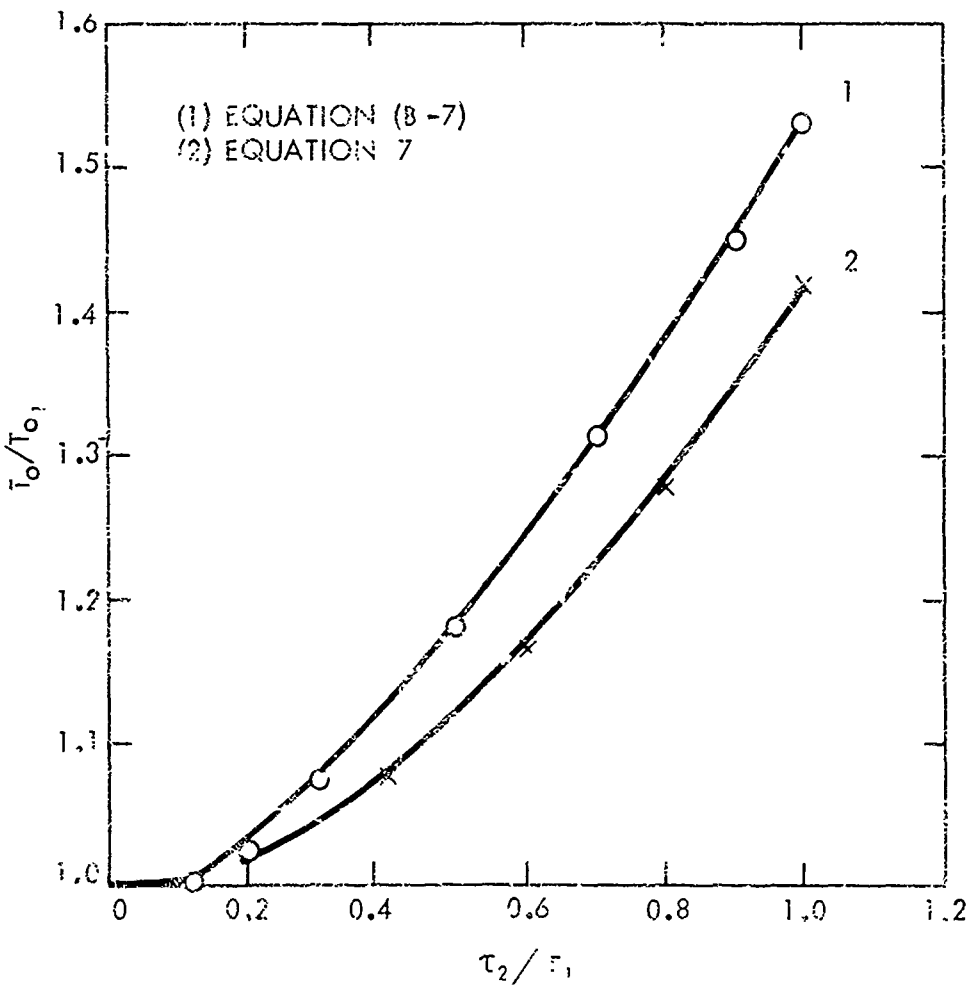

FIG. B-2 RELATIVE RISE TIME VS. TIME CONSTANT RATIO

APPENDIX C

WONDY CALCULATIONS IN PMMA

The WONDY Q Code[28] developed at the Sandia Corporation was used to generate particle velocity-time profiles which could be used to compare with results obtained by the EMV gage method. This code, which solves problems in one dimension, had been implemented for use at NOL[29]. The code was set up to simulate the LSGT configuration by using the spherical flow option. The solution is therefore an approximation to the real problem. In the code run the boundary between the HE and the PMMA is a radius equal to the height of the HE instead of a plane. The polytropic gas equation of state was used to describe the detonation products of the tetryl booster. A fluid equation of state was used for the PMMA. Equation (2) was used for the PMMA Hugoniot. These data were fitted to a relation between P and η, $\eta = 1 - \rho_o/\rho$, of the form

$$P = K_o\eta(1 + K_1\eta + K_2\eta^2) \quad ; \qquad \text{(C-1)}$$

the equation being treated as a general P-η relation. Parameters needed for the computation are listed in Table C-1.

The cell size chosen to limit the computing time to a reasonable value results in an effective rise time for the computations of about 225 ns. Consequently, as in the experiments, initial values of particle velocity at the shock front must be extrapolated. Particle velocity-time profiles on the particle paths for several values of X corresponding to the experiments reported here are plotted in Fig. (C-1). These results have been used in the text of this report to show the agreement with experiment. Agreement was quite good for $X \geq 4$ mm. The most significant difference between the computation and the experiment is the method of initiating the explosive for the computation. The explosive energy was released in the computation by using the burn fraction technique of the code. This method treats the reaction in an arbitrary way without a reaction zone. The comparative results for $X \leq 4$ mm would be most affected by this difference between computation and the real lighting event. The computated pressure at the interface was 153 kb which is in excellent agreement with the impedance value of 155 kb.

TABLE C-1

Parameters Used in WONDY Calculation

	Tetryl	PMMA
Cell length, cm	0.05	0.02
Number of cells	100	100
Rho_0, g/cm^3	1.51	1.18
C_0, mm/μsec	5.18	2.71
Gamma	2.82	
Detonation Velocity mm/μsec	7.2	
K_0		0.333
K_1		5.09
K_2		6.15

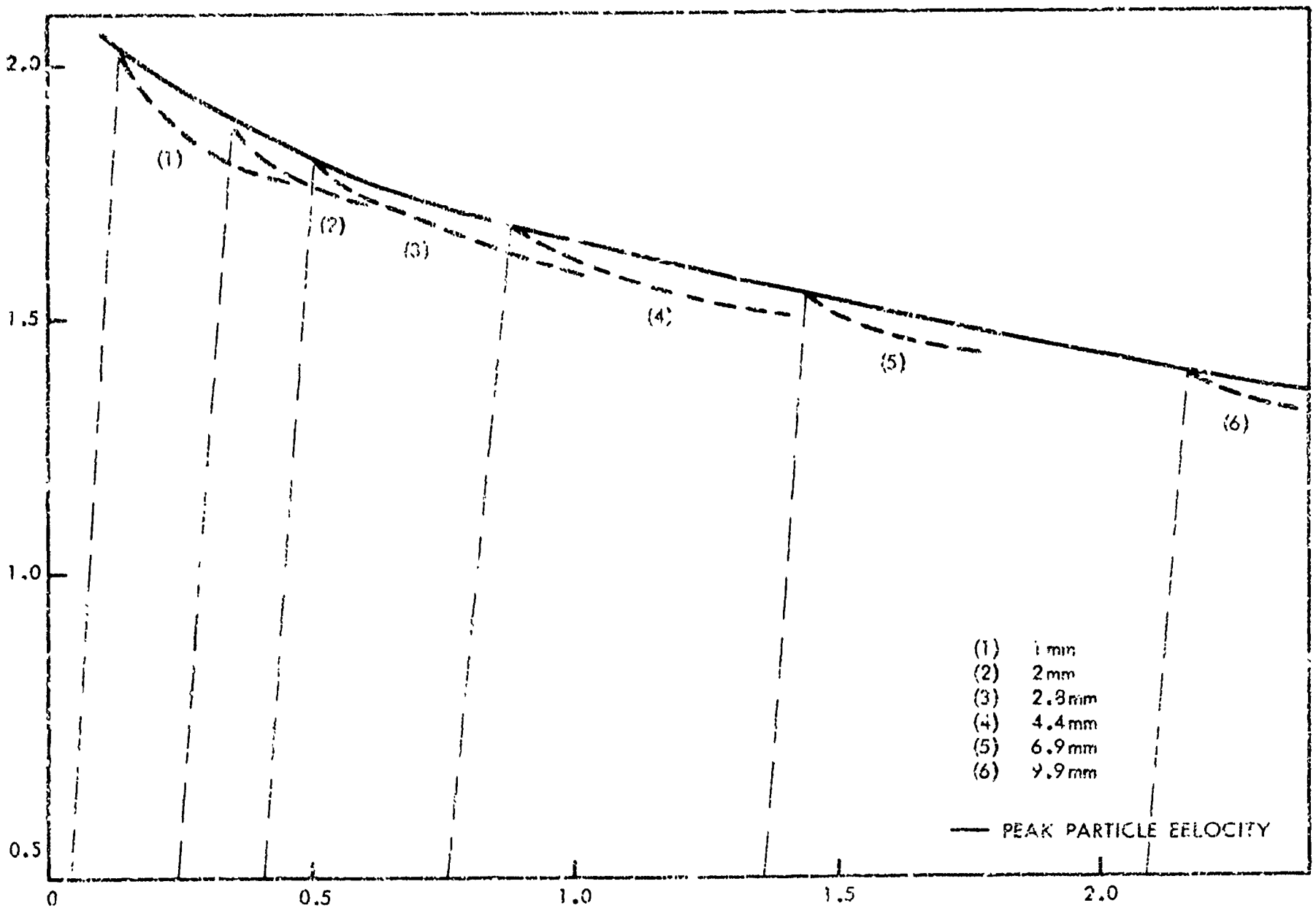

FIG. C-1 u - t RESULTS OBTAINED FROM WONDY CALCULATION

APPENDIX D

RESPONSE OF A SIMPLE RC NETWORK TO A DUAL SLOPE INPUT FUNCTION

At positions near to the interface in the simulated gap test experiment the expected particle velocity first decays quite rapidly and then levels off. A similar shape is expected in recording the particle velocity in a detonating explosive. It is known that the recording problem becomes difficult when the period of rapid decay in velocity is short. The following simplified problem should be of value in clarifying exactly what the response requirement should be. To illustrate the effect of recording system response, an input function to a simple RC network is taken to be a step jump followed first by a steeply decaying voltage linear in time. At a time t_1 the input is transferred to a new line of lesser slope. The response is computed for various values of the circuit time constant, $\tau = RC$, relative to t_1. Because of the sharp break in the input it is possible to clearly relate the response to the time constant. In actual practice the change in input slope may be much more gradual. It would probably be more difficult to distinguish such a change in slope in the output. The simplified problem is, nevertheless, expected to give a fair estimate to the required time constant relative to the time at which significant change in slope occurs.

The circuit used in this analysis is that of Appendix A. The input function illustrated in Fig. (D-1) can be expressed mathematically by the equation

$$e_0/e_{01} = 1 - k_j(t/t_1 - 1); \qquad (D\text{-}1)$$

where t_1 is the time at which the input changes from slope $k_j = k_0$ $k_j = k_1$. The quantity e_{01} is the input voltage at time t_1. The current in the circuit is given by the equation

$$e_0 = iR + \int (i/C)dt \quad . \qquad (D\text{-}2)$$

The solution to Eqs. (D-1) and (D-2) may be written in the form

$$iR/e_{01} = A_j \exp(-t/\tau) - k_j/t_1 \quad . \qquad (D\text{-}3)$$

The output of the circuit is given by

$$e/e_{01} = (e_0 - iR)/e_{01} \quad . \qquad (D\text{-}4)$$

Since we are interested in relative times and relative voltages it is useful to write the above equations in dimensionless form by using the following definitions. Define $y = t/t_1$, $\phi = \tau/t_1$, $Z = e/e_{01}$, and $Z_P = iR/e_{01}$. Equations above then become

$$Z_0 = 1 - k_j(y - 1) \quad , \tag{D-5}$$

$$Z_R = A_j \exp(-y/\phi) - k_j\phi \quad , \quad \text{and} \tag{D-6}$$

$$Z = Z_0 - Z_R \quad . \tag{D-7}$$

The initial value of A_j for $j = 0$ is determined from the fact that $Z = 0$ when $y = 0$. Therefore

$$A_0 = 1 + k_0 + k_0\phi \quad . \tag{D-8}$$

When $y = 1$, the value of A_1 is determined since Z_R must be continuous at the break point; that is

$$A_0 \exp(-1/\phi) - k_0\phi = A_1 \exp(-1/\phi) - k_1\phi$$

and

$$A_1 = A_0 - (k_0 - k_1)\phi \exp(1/\phi) \quad . \tag{D-9}$$

Equations (D-5) to (D-7) can be used in parametric form to compute the input and response. For y between 0 and 1 the subscript $j = 0$ values of k and A are used. For y equal to or greater than 1 the subscript $j = 1$ values are used. Illustrative solutions of the equations have been computed on the remote computer system of CEIR for $k_0 = 1$, $k_1 = 0.1$, and ϕ ranging from 0.1 to 2. The results are shown in Fig. (D-2). It is seen that the response shows no evidence of the inflection in the input when ϕ is 0.8 or greater. When ϕ is 0.1 the response shows the inflection very well yet the maximum in the curve falls about 15% short of the input value. Extrapolation of the initial part of the response to zero time gives a pretty good value for the initial value of the input when ϕ is 0.2 or less. It is to be expected that the response of a real recording system which comprises several RC circuits plus mechanical elements such as in the EMV gage system would show response behavior similar to that shown here. We would expect to find that the effective time constant of such a system could be defined in terms of an observed rise time, that is, $T_o \cong 2.2\ \tau$. In terms of rise time it appears that a rise time, T_o, would have to be less than half the time to an inflection point in order to get any information of significance concerning the initial steep portion of an input function from the signal which is recorded.

The problem solved above appeared to illustrate adequately the general features of recording response. Hence, no other problems with other values of k_j were tried. It should be noted that in Eqs. (D-7) and (D-6) the value of z tends toward $z_0 + k_j\emptyset$, when the output becomes linear. With the linear input the response, as can be seen in Fig. (D-1), is therefore shifted to the right by $\emptyset$. In principle, this implies that an extrapolation to obtain the initial particle velocity should be back to time $\emptyset$ rather than zero. In practice the difference due to ignoring this time shift is usually negligible. The correction was not made in the work reported here.

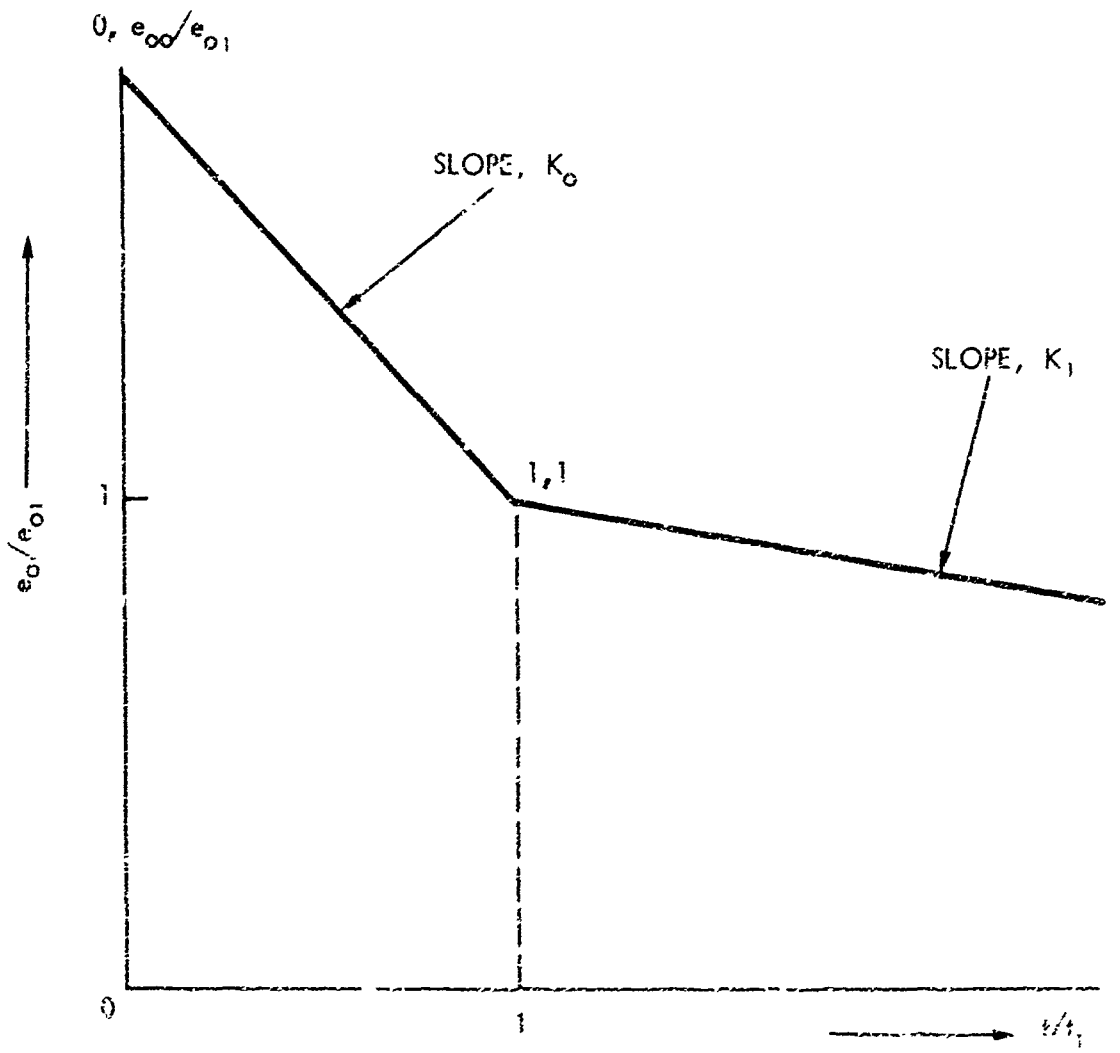

FIG. D-1 DOUBLE SLOPE INPUT FUNCTION

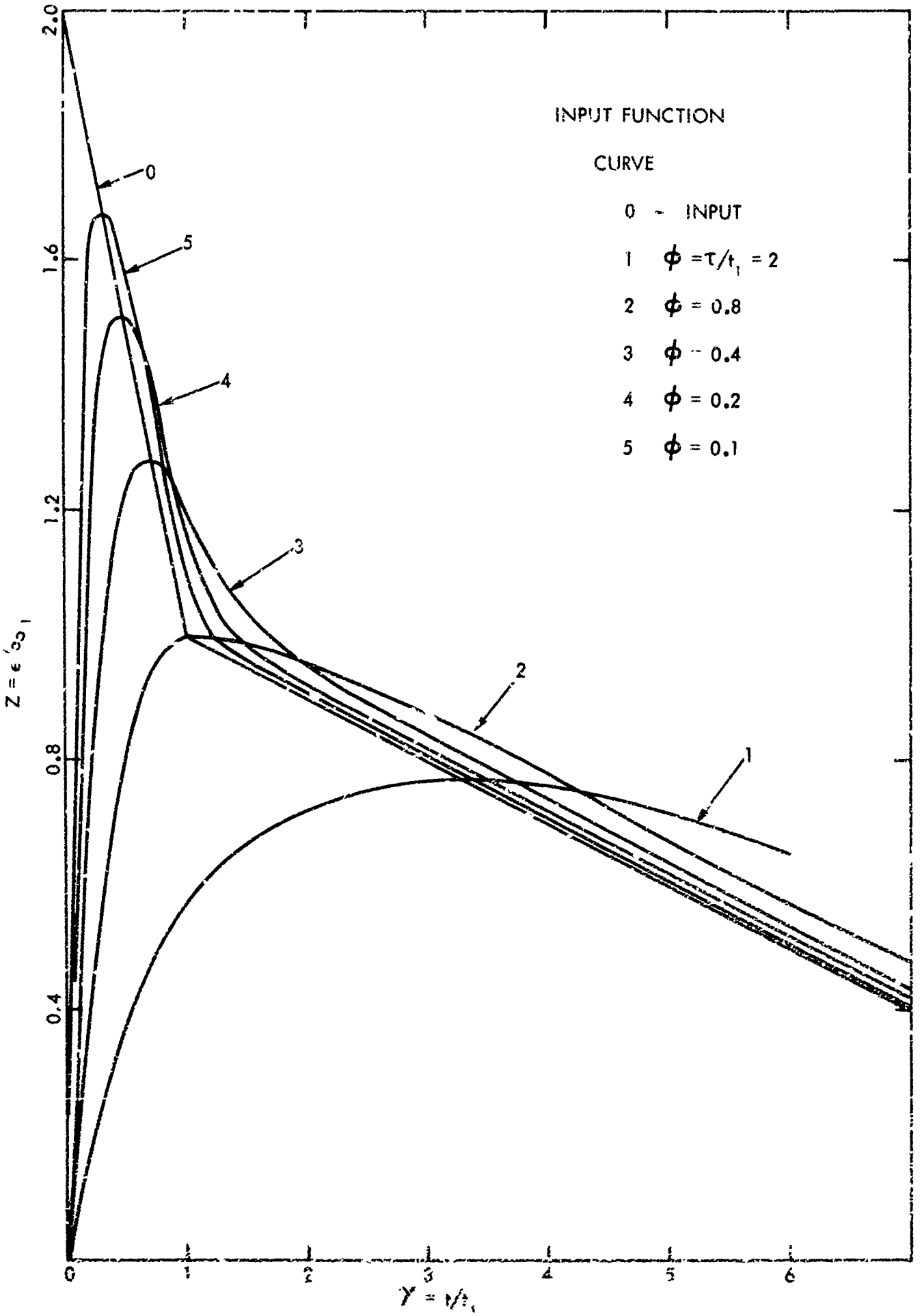

FIG. D-2 RESPONCE TO A 2 SLOPE

UNCLASSIFIED

Security Classification

DOCUMENT CONTROL DATA - R & D

Security classification of title, body of abstract and indexing annotation must be entered when the overall report is classified)

1 ORIGINATING ACTIVITY (Corporate author)

U. S. Naval Ordnance Laboratory
White Oak, Silver Spring, Md. 20910

2a. REPORT SECURITY CLASSIFICATION

UNCLASSIFIED

2b GROUP

3 REPORT TITLE

THE ELECTROMAGNETIC VELOCITY GAGE AND APPLICATIONS TO THE MEASUREMENT OF PARTICLE VELOCITY IN PMMA

4 DESCRIPTIVE NOTES (Type of report and inclusive dates)

5 AUTHOR(S) (First name, middle initial, last name)

David J. Edwards, John O. Erkman, and Sigmund J. Jacobs

6 REPORT DATE	7a. TOTAL NO OF PAGES	7b NO OF REFS
20 July 1970	48	29

8a CONTRACT OR GRANT NO	9a ORIGINATOR'S REPORT NUMBER(S)
MAT-03L-000/ZR011-01-01	NOLTR 70-79
b. PROJECT NO	
c.	9b OTHER REPORT NO'S) (Any other numbers that may be assigned this report)
d	

10 DISTRIBUTION STATEMENT

This document has been approved for public release and sale, its distribution is unlimited.

11 SUPPLEMENTARY NOTES	12 SPONSORING MILITARY ACTIVITY
	Naval Material Command

13 ABSTRACT

The electromagnetic velocity (EMV) gage was used to investigate particle velocity vs time and peak particle velocity vs distance at several points in PMMA (polymethylmethacrylate) in the donor-gap arrangement of the NOL Large Scale Gap Test. The results obtained by the method agree favorably with previously measured peak particle velocities for gap distances from the HE-PMMA interface between 10 and 25 mm. At closer distances the particle velocity-time records are in good relative agreement with one dimensional hydrodynamic computations. The values of peak particle velocity found for distances less than 5 mm are not in agreement with the previous extrapolation to zero gap of the earlier data obtained for gaps ≥ 10 mm. Consequently, a new tentative calibration for the close-in distance is presented. The study encountered a number of recording problems; noise in the records and poor system response. Steps taken to eliminate the noise and to improve the recording response are outlined. Also discussed are the theoretical behavior of the gage, factors influencing system response, and comparison of real with predicted response. It was concluded that the EMV gage is a convenient and useful tool for measuring particle velocity vs time in non-conducting or weakly conducting media.

( ) ← greater than or equal to

OR ≥

DD FORM 1 NOV 65 1473 (PAGE 1)

S/N 0101-807-6801

UNCLASSIFIED

Security Classification

14 KEY WORDS	LINK A		LINK B		LINK C	
	ROLE	WT	ROLE	WT	ROLE	WT
Electromagnetic Velocity Gage						
Particle velocity						
Large scale gap test						
Tetryl donor						
Calibration						